Naval Command,
Control and Ocean
Surveillance Center RDT&E Division San Diego, CA
92152-5000

(4)

Technical Report 1510
August 1992

Effects of CW- and BPSK-Signal Interference on a Standard BPSK Digital Communications System

R. A. Axford

NRaD

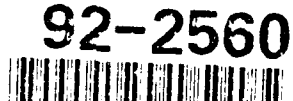

Technical Report 1510
August 1992

Effects of CW- and BPSK-Signal Interference on a Standard BPSK Digital Communications System

R. A. Axford

NAVAL COMMAND, CONTROL AND OCEAN SURVEILLANCE CENTER
RDT&E DIVISION
San Diego, California 92152-5000

J. D. FONTANA, CAPT, USN
Commanding Officer

R. T. SHEARER
Executive Director

ADMINISTRATIVE INFORMATION

This work was conducted during FY 1992 under project CG48. The work was performed for the Space and Naval Warfare Systems Command, Code 504P3, Washington, DC 20363-5100, and funded under program element 0603000N.

Released by
R. J. Nies, Head
Electro-Optic Systems
Branch

Under authority of
C. E. Gibbens, Head
Satellite Communications
Division

MA

SUMMARY

"The ultimate performance limitation of any communications system is susceptibility to interference. In the presence of interference, intentional or otherwise, the communicator, through signal processing at the transmitter and receiver, can ensure that performance degradation due to interference will be no worse than that caused by additive white Gaussian noise at equivalent power levels" (Viterbi, 1991).

To quantify the success of any scheme to mitigate the effects of interference, it is necessary to know what the effects of the interference are when the mitigating technique is not employed. This report contains calculations of the effects of continuous wave- (CW) and binary phase shift keyed- (BPSK) signal interferers on a standard BPSK communications system. These types of interferers are typical of those encountered in many BPSK communications systems.

CONTENTS

CONTENTS (continued)

FIGURES

CONTENTS (continued)

CONTENTS (continued)

TABLE

1.0 INTRODUCTION

In this report, the effects of two forms of interference on the error rate of a standard binary phase shift keyed (BPSK) digital communications system are examined. Specifically, the impacts of continuous wave- (CW) carrier and other BPSK-signal interferers on the probability of bit error in the matched-filter receiver of the standard BPSK communications system are calculated as functions of interferer-to-signal carrier power ratios, frequency offsets, phase offsets, and relative data rates. The term "standard" implies that no spread spectrum or forward error correction (FEC) coding techniques are employed in the BPSK system of interest.

In section 2, the probability of bit error, P_e, is derived for a matched-filter BPSK receiver operating in the presence of additive white Gaussian noise (AWGN) and no interfering signals. The receiver structure introduced in section 2 is used in all of the following sections.

In section 3, the effect of a CW interferer on P_e is calculated as a function of the interferer-to-signal carrier power ratio, J/S, and relative phase angles first, when the CW interferer frequency and the carrier frequency of the desired signal are identical. Then, the effects on P_e of varying the frequency of the CW interferer relative to the carrier frequency of the desired signal are also calculated for several values of J/S.

In section 4, the effects on P_e of an interfering BPSK signal are calculated as functions of the relative data rates of the interfering signal and the desired signal, the interferer-to-signal carrier power ratio, and the offset of the interferer-carrier frequency from that of the desired signal.

In section 5, the results of the previous sections are extended to the type of binary differential phase shift keying that is employed in the Navy ultrahigh frequency Fleet satellite communications (UHF FLTSATCOM) system: coherent detection of differentially encoded BPSK. An interesting interference-related consequence of the use of differential encoding is also examined.

In all of the calculations of the effects of the interferers on the bit-error probability of the standard BPSK communications system contained in this report, it is assumed the reference signal used for coherent demodulation of the received signal is not affected by the interference. In practice, since the reference signal is derived from the received signal by means of a carrier-tracking loop, the quality of the reference signal will be degraded by the interference when J/S is sufficiently high. As a consequence, the probability of error calculated here should be considered to be lower bounds on the probability of error performance of an actual standard BPSK communications system operating in the presence of CW- and BPSK-signal interferers. That is, the probability of error observed in practice will be higher than the results contained in this report, especially at the higher values of J/S where the quality of the reference signal is likely to be severely degraded.

2.0 MATCHED-FILTER DETECTION OF BPSK

The calculation of the probability of bit error for a BPSK system using a matched-filter receiver operating in the presence of AWGN and no other interference is well known (Milstein, 1991; Proakis, 1989; Sklar, 1988). The correlator implementation of a matched-filter receiver for BPSK is shown in figure 1. In the absence of interference, the received waveform $r(t)$ is given by

$$r(t) = \pm AP_t(t)\cos(\omega_c t) + n_w(t) \tag{1}$$

where

A = desired signal amplitude,

ω_c = desired signal-carrier frequency,

$P_T(t)$ is a rectangular pulse of unit height and duration T,

T = bit time $(1/R)$, and

$n_w(t)$ is additive white Gaussian noise with zero mean and variance $\frac{N_0}{2}$.

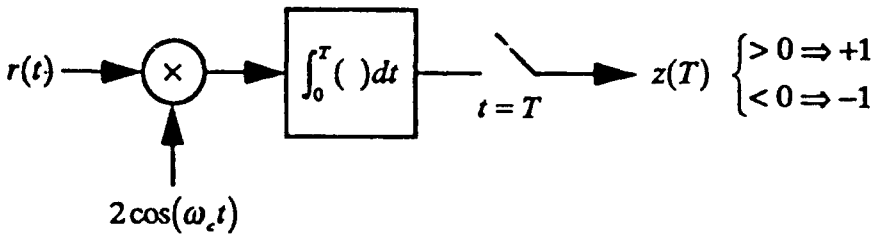

Figure 1. Correlator implementation of matched-filter receiver for BPSK.

The sign of the $AP_T(t)$ term depends on the value of the current data bit, corresponding to a carrier phase of 0 or 180 degrees. The quantity $z(T)$ in figure 1 is the test statistic and is given by

$$z(T) = \pm AT + 2\int_0^T n_w(t)\cos(\omega_c t)dt. \tag{2}$$

As indicated in figure 1, the value of $z(T)$ is compared to 0 at the end of each bit time. The receiver decides for +1 or −1 based on the polarity of $z(T)$. Now, because $n_w(t)$ is a zero mean Gaussian random process, $z(T)$ is a Gaussian random variable with conditional expected value, given the data, given by

$$E[z(T)|\ \pm 1] = \pm AT. \tag{3}$$

The variance σ_z^2 of $z(T)$ can be calculated under the assumption that no signal and only noise is present at the input of the receiver (Helstrom, 1984, p. 270). In this case, $E[z(T)] = 0$ and σ_z^2 is given by

$$\begin{aligned}
\sigma_z^2 &= E[z^2(T)] \\
&= 4\int_0^T dt_1 \int_0^T dt_2 E[n_w(t_1)n_w(t_2)]\cos(\omega_c t_1)\cos(\omega_c t_2) \\
&= 4\int_0^T dt_1 \int_0^T dt_2 \frac{N_0}{2}\delta(t_1 - t_2)\cos(\omega_c t_1)\cos(\omega_c t_2) \\
&= 2N_0 \int_0^T \cos^2(\omega_c t)dt \\
&= N_0 T.
\end{aligned} \tag{4}$$

An error is made if $z(T)$ has a polarity opposite that of the transmitted bit. Thus, assuming that +1 and −1 are equally likely, the probability P_e of bit error is given by

$$\begin{aligned}
P_e &= \frac{1}{2}\Pr[z(T) < 0|+1] + \frac{1}{2}\Pr[z(T) > 0|-1] \\
&= \frac{1}{2}\Phi\left(\frac{-AT}{\sqrt{N_0 T}}\right) + \frac{1}{2}\left\{1 - \Phi\left(\frac{AT}{\sqrt{N_0 T}}\right)\right\} \\
&= \Phi\left(\frac{-AT}{\sqrt{N_0 T}}\right) \\
&= \Phi\left(-\sqrt{\frac{A^2 T}{N_0}}\right) \\
&= \Phi\left(-\sqrt{\frac{2E_b}{N_0}}\right)
\end{aligned} \tag{5}$$

where $E_b = A^2T/2$ is the signal energy per bit, and

$$\Phi(x) = \frac{1}{\sqrt{2\pi}} \int_{-\infty}^{x} e^{-\frac{t^2}{2}} dt \tag{6}$$

is the cumulative normal distribution function. A plot of eq. (5) versus signal-to-noise ratio (SNR) = E_b/N_0 in dB is shown in figure 2.

In all of the following sections, the desired signal will have random BPSK modulation with an SNR of 10 dB. From figure 2, $P_e \approx 4 \times 10^{-6}$ for a standard BPSK system when SNR = 10 dB. A desired signal-data rate R = 2400 bps is also used in all calculations, which results in a desired signal carrier-to-noise density ratio C/N_0 of 43.8 dBHz.

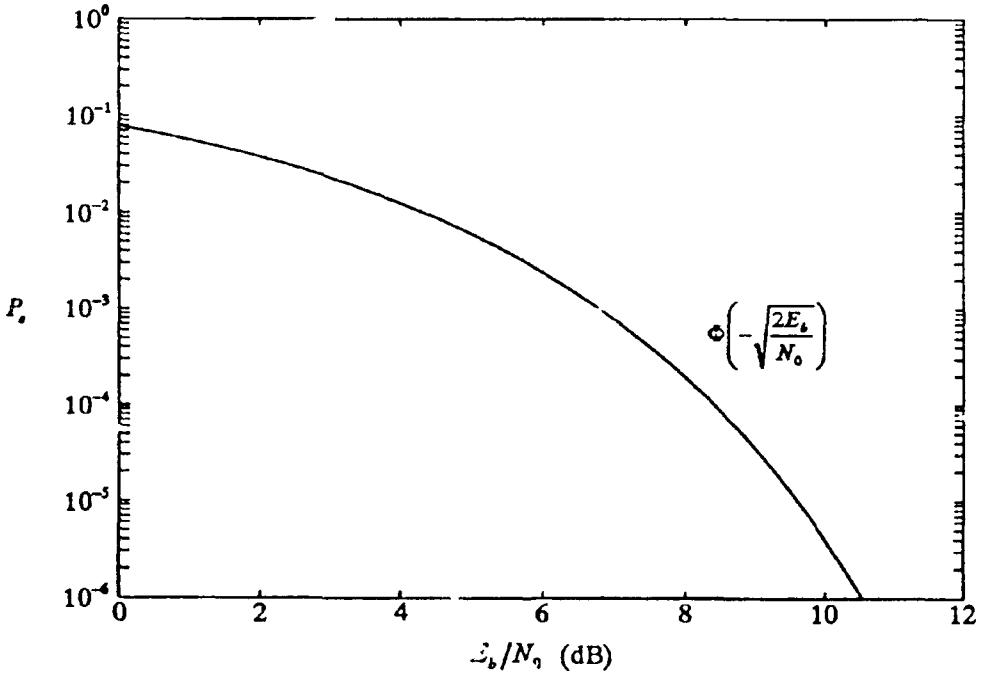

Figure 2. BPSK: Probability of bit error P_e vs. E_b/N_0, no interference.

3.0 CW CARRIER INTERFERER

In this section, the impact of a CW carrier interferer on the error rate of the standard BPSK system is calculated as a function of the ratio J/S of interferer-to-signal carrier power, the carrier phase offset of the CW interferer with respect to the desired signal carrier when the signals are centered at the same frequency, and the carrier-frequency offset when the two signals are not centered at the same frequency.

3.1 DESIRED SIGNAL, INTERFERER, AND NOISE MODEL

The model of the received waveform, $r(t)$, used in this section is given by

$$r(t) = \pm AP_T(t)\cos(\omega_c t) + a\cos[(\omega_c + \delta)t + \theta] + n_w(t) \tag{7}$$

where

A = desired signal amplitude,

a = interferer amplitude,

ω_c = desired signal-carrier frequency,

δ = interferer–frequency offset,

θ = interferer phase,

$P_T(t)$ is a rectangular pulse of unit height and duration T,

T = bit time $(1/R)$, and

$n_w(t)$ is additive white Gaussian noise with zero mean and variance $\frac{N_0}{2}$.

The interfering signal consists of a single CW carrier offset by δ Hz from the desired signal-carrier frequency. Assuming coherent demodulation and matched-filter detection as shown in figure 1, the test statistic, $z(T)$, at the end of each bit time is given by

$$z(T) = \pm AT + a\int_0^T \cos(\delta t + \theta)dt + 2\int_0^T n_w(t)\cos(\omega_c t)dt. \tag{8}$$

Again, $z(T)$ is a Gaussian random variable with variance σ_z^2 given by

$$\sigma_z^2 = N_0 T. \tag{9}$$

The conditional expected value of $z(T)$, given the interferer amplitude, frequency, and phase, is given by

$$E[z(T)|a,\delta,\theta] = \pm AT + \frac{a\cos\theta}{\delta}\sin\delta T + \frac{a\sin\theta}{\delta}[\cos\delta T - 1]. \quad (10)$$

In general then, the probability P_e of bit error of a BPSK system operating in the presence of a CW carrier interferer with arbitrary amplitude, frequency, and phase, is given by

$$P_e(a,\delta,\theta) = \frac{1}{2}\Phi\left[\frac{-\left(AT + \frac{a\cos\theta}{\delta}\sin\delta T + \frac{a\sin\theta}{\delta}[\cos\delta T - 1]\right)}{\sqrt{N_0 T}}\right] + \frac{1}{2}\Phi\left[\frac{-\left(AT - \frac{a\cos\theta}{\delta}\sin\delta T - \frac{a\sin\theta}{\sigma}[\cos\delta T - 1]\right)}{\sqrt{N_0 T}}\right] \quad (11)$$

3.2 INTERFERER FREQUENCY THE SAME AS THE DESIRED SIGNAL-CARRIER FREQUENCY

If the interferer's frequency is the same as that of the desired signal, then, taking the limit of eq. (10) as δ goes to zero yields

$$\lim_{\delta \to 0} E[z(T)|a,\sigma,\theta] = \pm AT + aT\cos\theta. \quad (12)$$

In this case, the conditional probability of bit error, given a and θ, is given by

$$P_e(a,\theta) = \frac{1}{2}\Phi\left(\frac{-T(A + a\cos\theta)}{\sqrt{N_0 T}}\right) + \frac{1}{2}\Phi\left(\frac{-T(A - a\cos\theta)}{\sqrt{N_0 T}}\right) \quad (13)$$

3.2.1 Deterministic Interferer Phase

If the phase of the interferer with respect to the desired signal's carrier is fixed, then the worst possible case occurs when $\theta = 0$ or $\theta = 180$ degrees. When the interferer is exactly ±90 degrees out of phase with the BPSK carrier, it has no effect on $P_e(a,\theta)$ if the receiver being used is equivalent to that shown in figure 1. A plot of eq. (13) for the case of $\theta = 0$ degrees is shown in figure 3 for values of interferer-to-signal ratio J/S, defined as

$$J/S = 20\log_{10}(a/A), \quad (14)$$

ranging from -40 to +10 dB. Plots of eq. (13) versus θ for four values of J/S (-20, -10, -5, and 0 dB) are shown in figure 4.

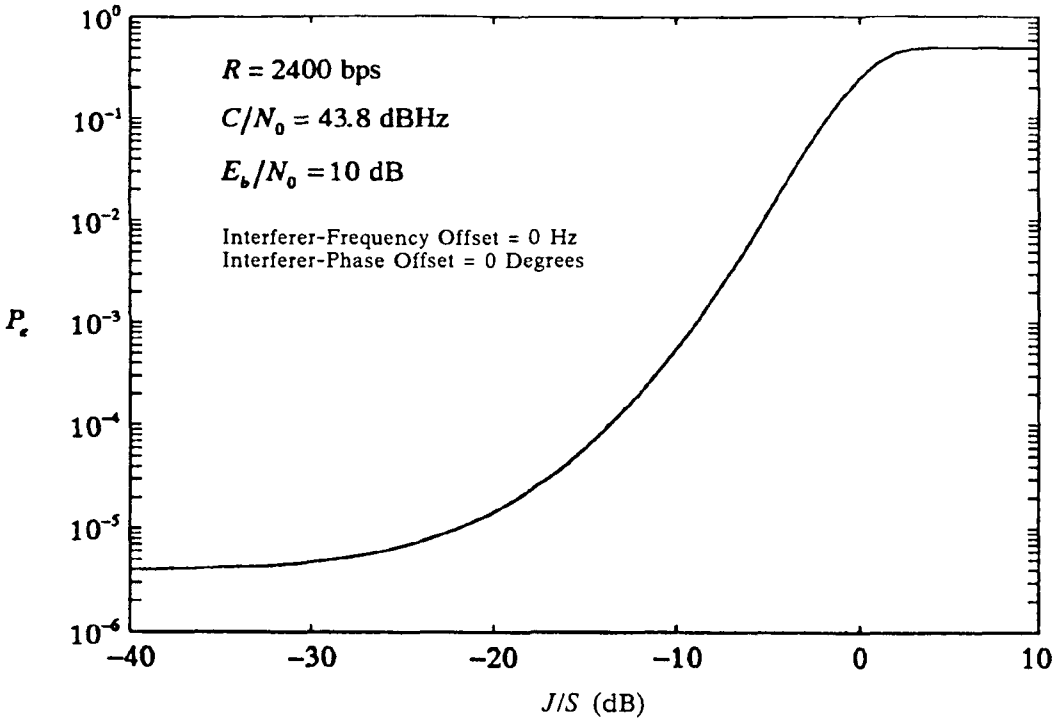

Figure 3. Probability of bit error vs. CW interferer-to-signal carrier power ratio, θ = 0.

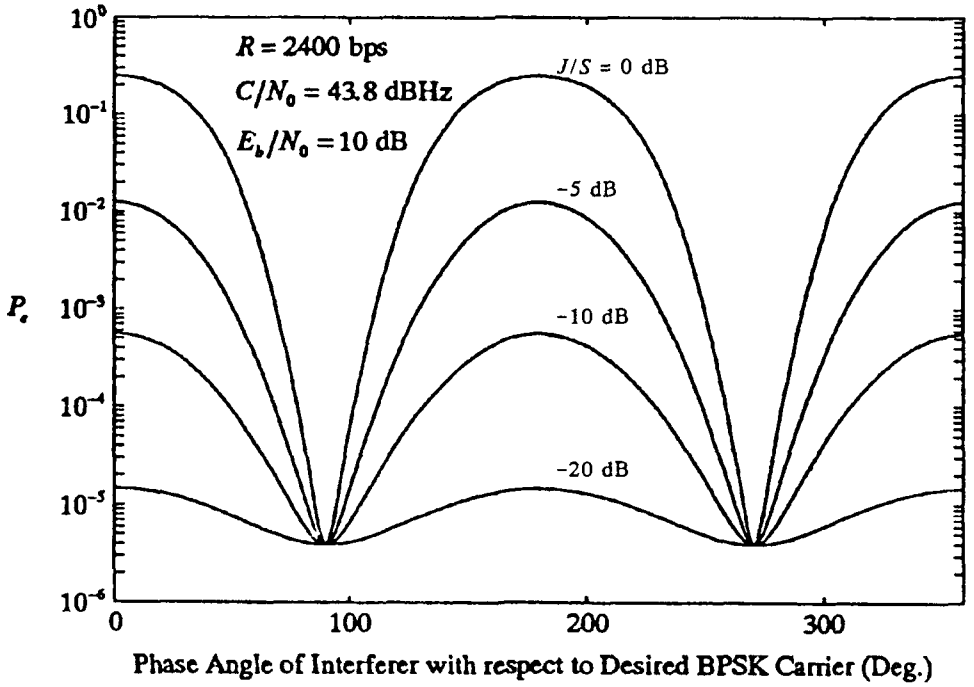

Figure 4. Probability of bit error vs. CW interferer-phase angle, J/S = 0, −5, −10, −20 dB.

3.2.2 Random Interferer Phase

It will most often be the case that the frequency of the CW interferer will not exactly match the carrier frequency of the desired signal. Thus, the phase angle of the CW interferer with respect to that of the desired signal will drift with time. When there is no reason for any particular value of phase to be preferred over any other, it should be assumed that θ is a random variable uniformly distributed on the interval $[0, 2\pi]$. In this case, the probability $P_e(a, \delta)$ of bit error is obtained from $P_e(a, \delta, \theta)$ by removing the conditioning on θ as follows (Milstein, 1991)

$$P_e(a, \delta) = \int_0^{2\pi} \frac{1}{2\pi} P_e(a, \delta, \theta) d\theta. \tag{15}$$

The integral in eq. (15) can be evaluated numerically. A plot of eq. (15) as a function of J/S for the case $\delta = 0$ is shown in figure 5, which also contains a plot of eq. (13) with $\theta = 0$ as in figure 3 for comparison. When averaged over all possible phase angles, the probability of bit error is slightly less at most values of J/S. At smaller values of J/S, the interferer makes little difference in P_e so its phase angle relative to that of the desired signal becomes irrelevant.

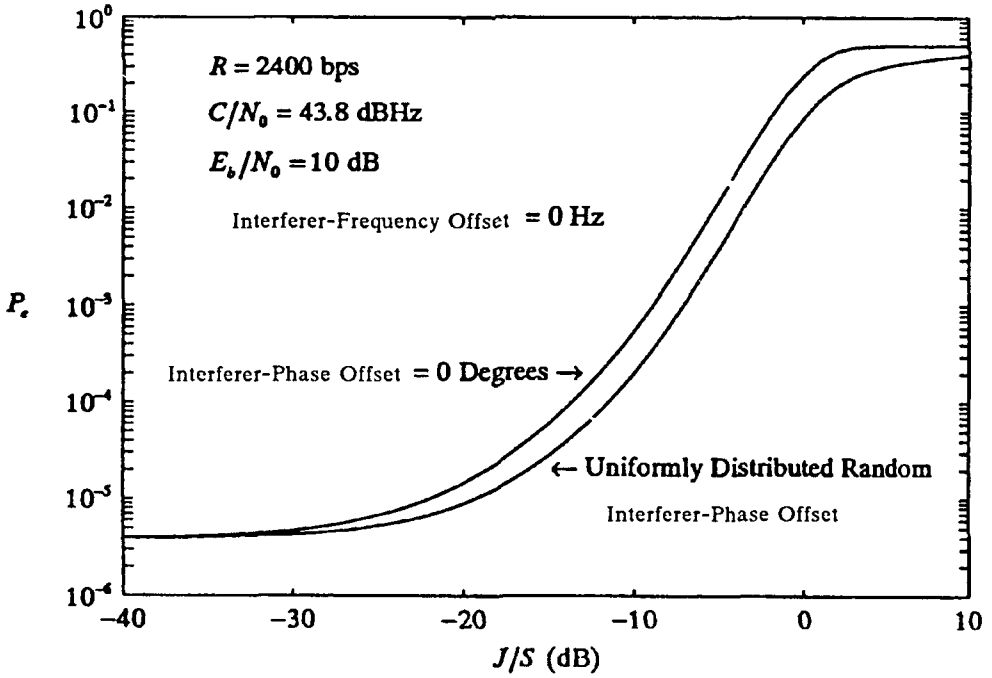

Figure 5. Probability of bit error vs. CW interferer-to-signal carrier power ratio, $\theta = 0$ and θ random.

3.3 CW INTERFERER FREQUENCY DIFFERENT FROM THE DESIRED SIGNAL-CARRIER FREQUENCY

In this section, the effect of the CW interferer-frequency offset δ on the probability of bit error is examined. In figure 6, $P_e(a, \delta)$ is plotted as a function of δ for five values of J/S. In each case, the interferer's phase angle was taken to be uniformly distributed over $[0, 2\pi]$ and the integration indicated in eq. (15) was performed numerically at each value of δ. As might be expected, the stronger the CW interferer, the larger δ can be for significant degradation of P_e to occur. For J/S = −10 dB, the interferer's frequency must be within the main lobe of the spectrum of the desired BPSK signal to cause an order of magnitude degradation of P_e. When J/S = +10 dB, an interferer that is offset by 4.5 times the data rate from the carrier frequency of the desired signal will increase P_e by slightly more than an order of magnitude. In all cases, a CW interferer whose frequency coincides with a zero in the spectrum of the desired BPSK signal has no effect on P_e.

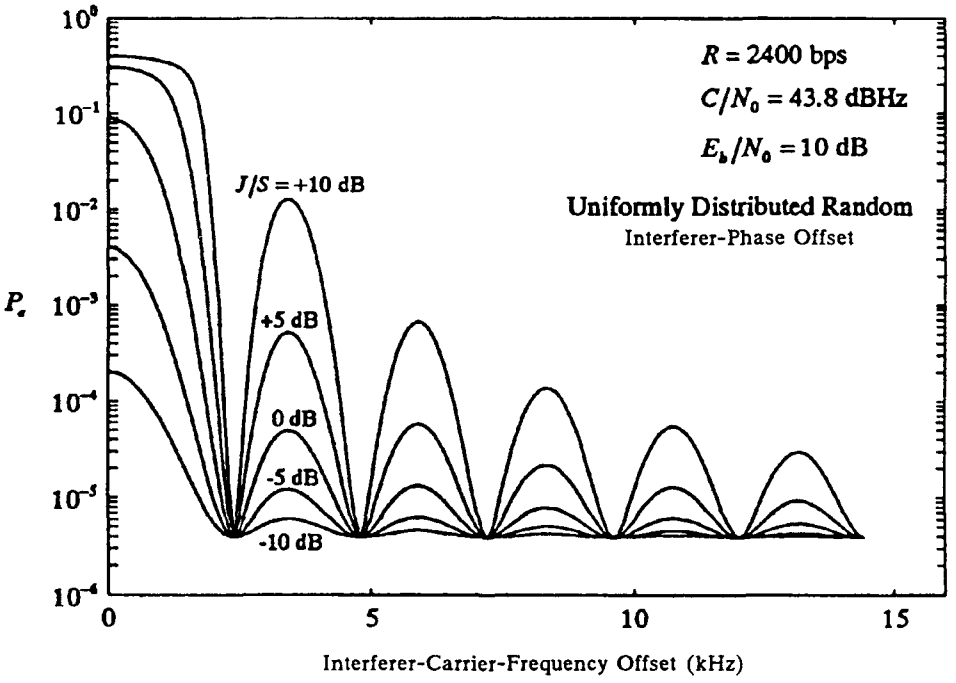

Figure 6. Probability of bit error vs. CW interferer-frequency offset, J/S = +10, +5, 0, −5, and −10 dB, θ random.

4.0 INTERFERING BPSK SIGNAL

In this section, the impact of an interfering BPSK signal on the bit-error rate of the standard BPSK system of interest is calculated as a function of the relative data rates of the two signals, the ratio J/S of interferer-to-signal carrier power, and the carrier frequency offset when the two signals are not centered at the same frequency.

4.1 DESIRED SIGNAL, INTERFERING SIGNAL, AND NOISE MODEL

The model of the received waveform, $r(t)$, used in this section is similar to that in eq. (7) except that the CW interferer is replaced by an interfering BPSK signal. Thus,

$$\begin{aligned} r(t) &= \pm AP_T(t)\cos(\omega_c t) \\ &\quad + A_I \sum_{k=-1}^{L} d_k P_{T_I}(t - kT_I - \tau)\cos[(\omega_c + \delta)t + \theta] \\ &\quad + n_w(t) \end{aligned} \tag{16}$$

where

A = desired signal amplitude,

A_I = interfering signal amplitude,

ω_c = desired signal–carrier frequency,

δ = interfering signal–carrier–frequency offset,

θ = interfering signal phase,

$P_T(t)$ is a rectangular pulse of unit height and duration T,

T = bit time $(1/R)$ of the desired signal,

T_I = bit time $(1/R_I)$ of the interfering signal,

τ = bit transition time offset, $\tau = \beta \min(T, T_I)$, $0 \le \beta < 1$,

d_k = ± 1, the data bits in the interfering signal, and

$n_w(t)$ is additive white Gaussian noise with zero mean and variance $\frac{N_0}{2}$.

It is assumed that $R_I = 2^n R$, where n is an element of [..., -2, -1, 0, 1, 2, ...]. The upper limit L of the sum in the interfering BPSK signal term is determined by the relative data rates and is given by

$$L = \begin{cases} 0, & n \leq 0 \\ 2^n - 1, & n > 0 \end{cases} \tag{17}$$

When $n < 0$, there will be some bit intervals in which no interfering signal bit transitions occur. In these cases, the interfering BPSK signal component of $r(t)$ in $[0, T]$ is simply $\pm A_I \cos[(\omega_c + \delta)t + \theta]$, which is equivalent to the component due to a CW interferer in eq. (7) with α replaced by A_I.

In general, the test statistic is given by

$$\begin{aligned} z(T) = \pm AT + A_I \int_0^T \left\{ \sum_{k=-1}^{L} d_k P_{T_I}(t - kT_I - \tau)\cos[\delta t + \theta] \right\} dt \\ + 2\int_0^T n_w(t)\cos(\omega_c t)dt \end{aligned} \tag{18}$$

when the matched-filter receiver of figure 1 is used. Again, $z(T)$ is a Gaussian random variable with variance $\sigma_z^2 = N_0 T$.

4.2 EQUAL OR LOWER DATA RATE BPSK INTERFERER

When $R_I \leq R$, there can be at most one bit transition of the interfering BPSK signal during any interval $[0, T]$. When such a transition does occur, the received signal in $[0, T]$ is given by

$$\begin{aligned} r(t) = \pm AP_T(t)\cos(\omega_c t) \\ + A_I\{d_{-1}P_{T_I}(t + T_I - \tau) + d_0 P_{T_I}(t - \tau)\}\cos[(\omega_c + \delta)t + \theta] \\ + n_w(t) \end{aligned} \tag{19}$$

This is shown at baseband in figure 7 for the case $d_{-1} = -1$ and $d_0 = +1$. The amplitude A_{IB} of the interfering baseband component is determined by the values of A_I, δ and θ in eq. (16).

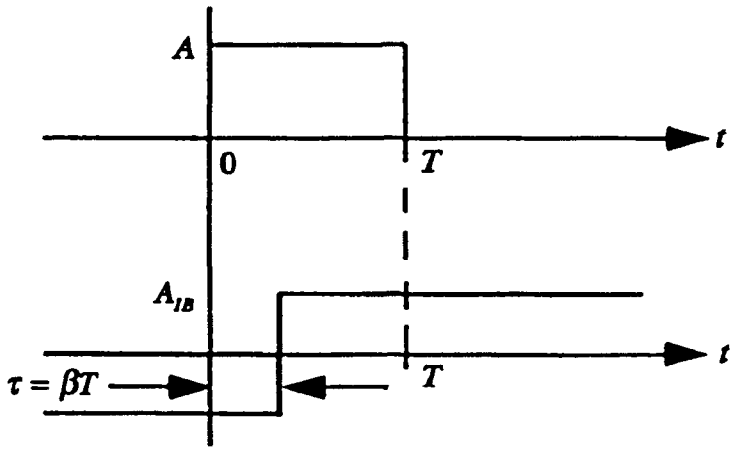

Figure 7. Desired (top) and interfering baseband signals in $[0, T]$, $R_I < R$, $d_{-1} = -1$ and $d_0 = +1$. $\tau = \beta T$, $0 \le \beta < 1$.

The conditional expected value of the test statistic in this case is given by

$$\begin{aligned} E[z(T)|A_I, \delta, \tau, \theta] &= \pm AT \pm A_I \int_0^{\tau} \cos[\delta t + \theta] dt \pm \int_{\tau}^{T} \cos[\delta t + \theta] dt \\ &= \pm AT \pm A_I K_1(\delta, \tau, \theta) \pm A_I K_2(\sigma, \tau, \theta) \end{aligned} \tag{20}$$

where

$$\begin{aligned} K_1(\delta, \tau, \theta) &= \frac{\cos\theta}{\delta} \sin\delta\tau + \frac{\sin\theta}{\delta}[\cos\delta\tau - 1] \\ K_2(\delta, \tau, \theta) &= \frac{\cos\theta}{\delta}[\sin\delta T - \sin\delta\tau] + \frac{\sin\theta}{\delta}[\cos\delta T - \cos\delta\tau] \end{aligned} \tag{21}$$

Given that the current data bit in the desired signal is +1, the conditional probability of bit error is given by (dropping the arguments of K_1 and K_2)

$$\begin{aligned} P_e(+1, A_I, \delta, \tau, \theta) &= \frac{1}{4}\Pr(z(T) < 0 | d_{-1} = -1, d_0 = -1) \\ &+ \frac{1}{4}\Pr(z(T) < 0 | d_{-1} = -1, d_0 = +1) \\ &+ \frac{1}{4}\Pr(z(T) < 0 | d_{-1} = +1, d_0 = -1) \\ &+ \frac{1}{4}\Pr(z(T) < 0 | d_{-1} = +1, d_0 = +1) \\ &= \frac{1}{4}\Phi\left(\frac{-AT + A_I K_1 + A_I K_2}{\sqrt{N_0 T}}\right) + \frac{1}{4}\Phi\left(\frac{-AT + A_I K_1 - A_I K_2}{\sqrt{N_0 T}}\right) \\ &= \frac{1}{4}\Phi\left(\frac{-AT - A_I K_I + A_I K_2}{\sqrt{N_0 T}}\right) + \frac{1}{4}\Phi\left(\frac{-AT - A_I K_1 - A_I K_2}{\sqrt{N_0 T}}\right). \end{aligned} \tag{22}$$

If the current bit in the desired signal is −1, then the conditional probability of error is given by

$$\begin{aligned} P_e(-1, A_I, \delta, \tau, \theta) &= \frac{1}{4}\Pr(z(T) > 0 | d_{-1} = -1, d_0 = -1) \\ &+ \frac{1}{4}\Pr(z(T) > 0 | d_{-1} = -1, d_0 = +1) \\ &+ \frac{1}{4}\Pr(z(T) > 0 | d_{-1} = +1, d_0 = -1) \\ &+ \frac{1}{4}\Pr(z(T) > 0 | d_{-1} = +1, d_0 = +1) \\ &= \frac{1}{4}\Phi\left(\frac{-AT - A_I K_1 - A_I K_2}{\sqrt{N_0 T}}\right) + \frac{1}{4}\Phi\left(\frac{-AT - A_I K_1 + A_I K_2}{\sqrt{N_0 T}}\right) \\ &+ \frac{1}{4}\Phi\left(\frac{-AT + A_I K_1 - A_I K_2}{\sqrt{N_0 T}}\right) + \frac{1}{4}\Phi\left(\frac{-AT + A_I K_1 + A_I K_2}{\sqrt{N_0 T}}\right) \end{aligned} \tag{23}$$

Thus, when there is an interfering signal bit transion in $[0, T]$, the conditional probability of error, given the parameters of the interfering signal, is given by

$$P_e(A_I, \delta, \tau, \theta) = \frac{1}{2}P_e(+1, A_I, \delta, \tau, \theta) + \frac{1}{2}P_e(-1, A_I, \delta, \tau, \theta). \tag{24}$$

Examination of the terms in eqs. (22) and (23) reveals that

$$P_e(+1, A_I, \delta, \tau, \theta) = P_e(-1, A_I, \delta, \tau, \theta). \tag{25}$$

Thus,

$$P_e(A_I, \delta, \tau, \theta) = P_e(+1, A_I, \delta, \tau, \theta) = P_e(-1, A_I, \delta, \tau, \theta). \tag{26}$$

Over several desired signal bit intervals, the fraction γ of them in which interfering signal bit transitions do occur is given by

$$\gamma = R_I/R. \tag{27}$$

In the desired signal bit intervals that do not contain interfering signal bit transitions, the conditional probability of error is given by eq. (26) evaluated at $\tau = 0$ which reduces to the CW interferer result in eq. (11) with α replaced by A_I. On the average then, when $R_I \leq R$ the conditional probability of bit error is given by

$$P_e(A_I, \delta, \tau, \theta, \gamma) = \gamma P_e(A_I, \delta, \tau, \theta) + (1-\gamma) P_e(A_I, \delta, 0, \theta). \tag{28}$$

As in eq. (15), the probability $P_e(A_I, \delta, \gamma)$ of bit error can be calculated by averaging out the dependence on both θ and τ as follows

$$P_e(A_I, \delta, \gamma) = \gamma \frac{1}{2\pi}\frac{1}{T}\int_0^{2\pi} d\theta \int_0^T d\tau P_e(A_I, \delta, \tau, \theta) + (1-\lambda)\frac{1}{2\pi}\int_0^{2\pi} d\theta P_e(A_I, \delta, 0, \theta) \tag{29}$$

where θ and τ have been assumed to be mutually dependent and uniformly distributed on $[0, 2\pi]$ and $[0, T]$ respectively. As $\gamma \rightarrow 0$, the error rate degradation in the presence of the interfering BPSK signal approaches that caused by a CW interferer of equal carrier power as intuition predicts.

4.2.1 Interferer-Carrier Frequency the Same as the Desired Signal-Carrier Frequency

Taking the limit of eq. (21) as the carrier-frequency offset δ goes to zero yields

$$\begin{aligned} \lim_{\delta \rightarrow 0} K_1(\delta, \tau, \theta) &= \tau \cos\theta. \\ \lim_{\delta \rightarrow 0} K_2(\delta, \tau, \theta) &= (T - \tau) \cos\theta. \end{aligned} \tag{30}$$

But $\tau = \beta T$ where $0 \leq \beta < 1$. Thus, the conditional expected value of the test statistic is (replacing τ with β in the arguments)

$$\lim_{\delta \rightarrow 0} E[z(T)|A_I, \delta, \beta, \theta] = \pm AT + A_I T[\pm \beta \pm (1-\beta)]\cos\theta. \tag{31}$$

Thus, when there is an interfering signal bit transition in $[0, T]$, the conditional probability of bit error is given by

$$\begin{aligned} P_e(A_I, \beta, \theta) = {} & \frac{1}{4}\Phi\left(\frac{-T(A + A_I\cos\theta)}{\sqrt{N_0 T}}\right) + \frac{1}{4}\Phi\left(\frac{-T(A - A_I\cos\theta)}{\sqrt{N_0 T}}\right) \\ & + \frac{1}{4}\Phi\left(\frac{-T(A + A_I[2\beta - 1]\cos\theta)}{\sqrt{N_0 T}}\right) + \frac{1}{4}\Phi\left(\frac{-T(A - A_I[2\beta - 1]\cos\theta)}{\sqrt{N_0 T}}\right) \end{aligned} \tag{32}$$

When there is not an interfering signal bit transition in $[0, T]$, $\beta = 0$ and eq. (32) reduces to the CW interferer result in eq. (13) with a replaced by A_I. Again, the worst possible situation for the system of interest would occur when $\theta = 0$ or 180 degrees. Defining the interferer-to-signal carrier power ratio J/S here as

$$J/S = 20\log_{10}(A_I/A), \tag{33}$$

the plot of P_e versus J/S for CW interference shown in figure 3 also applies to eq. (32) with $\beta = \theta = 0$. The plot of P_e versus J/S for CW interference shown in figure 5 also applies to eq. (32) when $\beta = 0$ and θ is considered to be uniformly distributed on $[0, 2\pi]$ and the dependence on θ is averaged out as in eqs. (29) or (15).

If there is an interfering signal bit transition in $[0, T]$, then $0 < \beta < 1$ in eq. (32) (see figure 7). Figure 8 shows plots of P_e versus β calculated with eq. (32) for $\theta = 0$, the worst case situation, at four values of J/S. When $\beta = 1/2$, the interfering signal bit transition occurs halfway through $[0, T]$ and P_e is reduced by roughly 1/2 for the higher

J/S ratios as expected.[1] The curves in figure 8 illustrate that, in the case of identical carrier frequencies, the degradation of desired system-bit-error rate caused by an equal or lower data rate interfering BPSK signal varies by at most a factor of 2 as R_I is reduced from R to zero. If the data rate of the interferer is zero, then it becomes a CW interferer. As a result, the curves in figure 5 give upper bounds, that are within a factor of 2, on the probability of bit error in the presence of an equal or lower data rate interfering BPSK signal on the same carrier frequency as the desired BPSK signal.

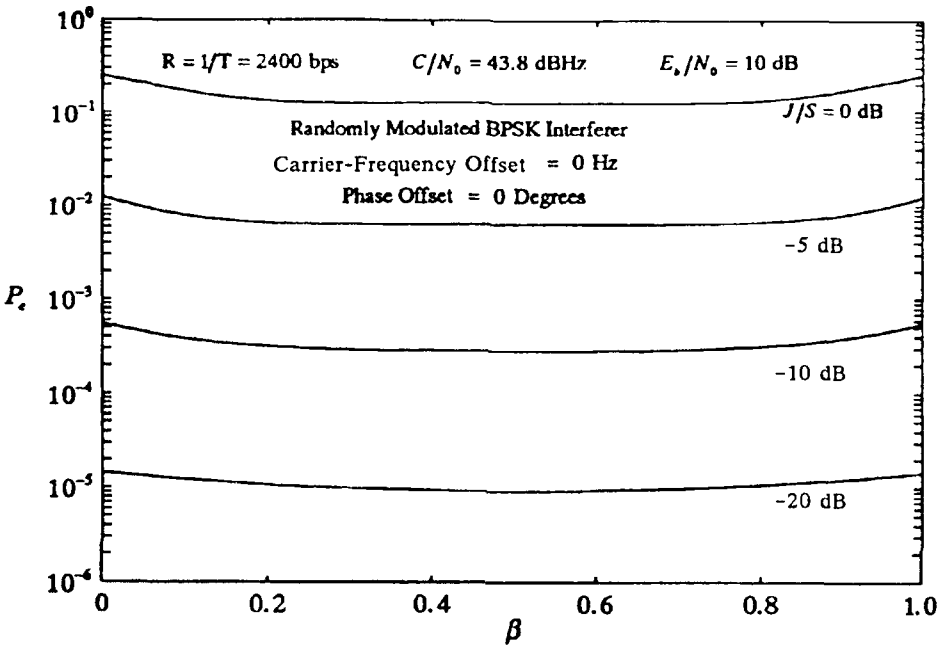

Figure 8. Probability of bit error as a function of the position of a single interfering signal bit transition in $[0, T]$. $\beta = \tau/T$ (see also figure 7). J/S = 0, -5, -10, -20 dB.

4.2.2 Interferer-Carrier Frequency Different from the Desired Signal-Carrier Frequency

Figures 9 through 15 contain plots of eq. (29) evaluated for interferer-data rates of 2400, 1200, 600, 300, 150, 75, and 0 bps respectively, when the interferer-carrier-frequency offset $\delta \neq 0$. In all cases, the desired signal-data rate is 2400 bps. Each figure contains a plot of eq. (29) for each of five values of J/S: +10, +5, 0, -5, and -10 dB. The integrations indicated in eq. (29) were performed numerically for each value of δ. In figure 15, since the interferer-data rate is 0 bps, the effect on the error probability is identical to that shown for a CW interferer in figure 6.

[1]With regard to the possible combinations of interfering signal bits, when $\beta = 0$, there are two possible outcomes, one of which will most likely cause an error. When $\beta = 1/2$, there are four possible outcomes, of which only one will most likely cause an error.

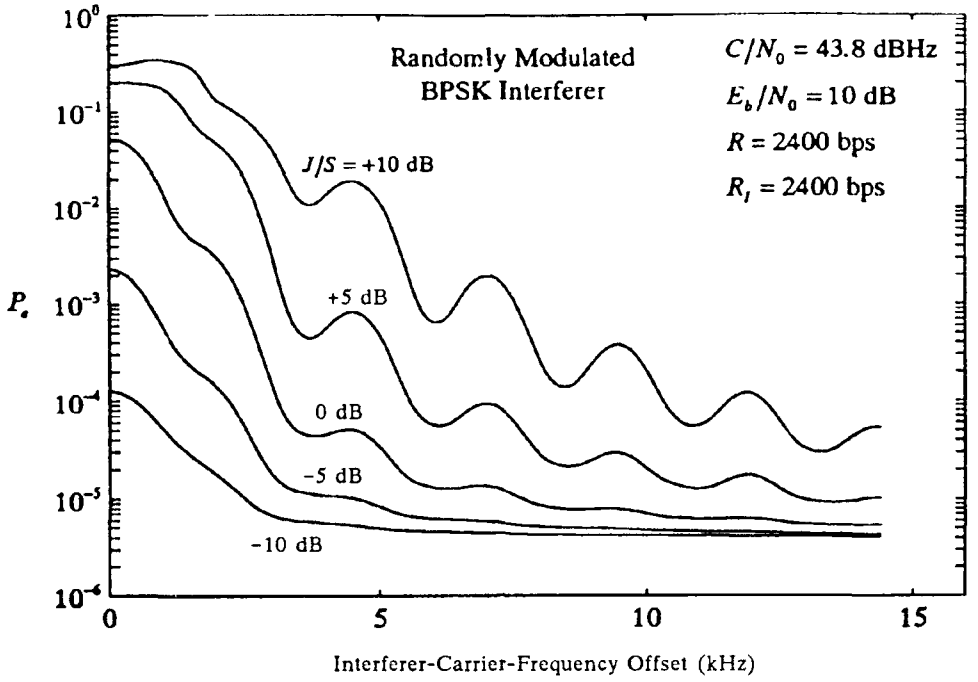

Figure 9. Probability of bit error vs. interferer-carrier-frequency offset, $R_I = R$.

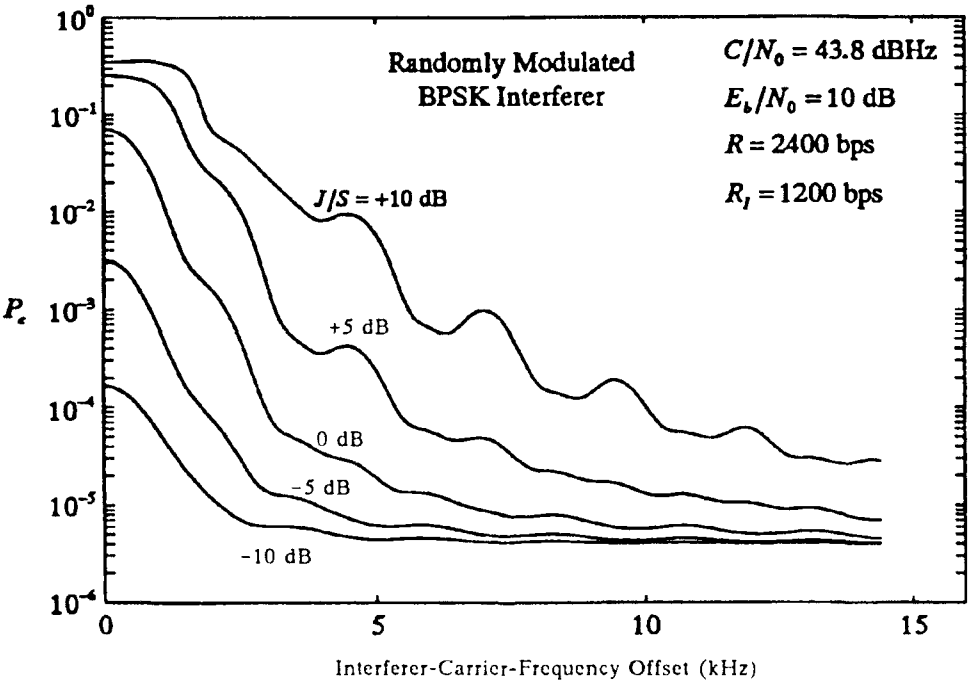

Figure 10. Probability of bit error vs. interferer-carrier-frequency offset, $R_I = R/2$.

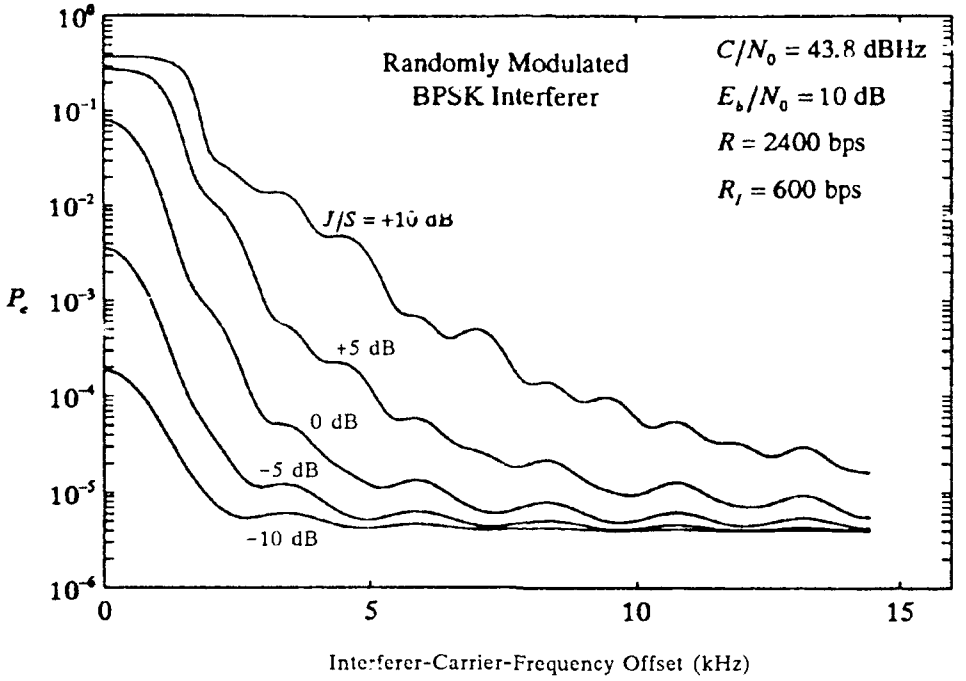

Figure 11. Probability of bit error vs. interferer-carrier-frequency offset, $R_I = R/2^2$.

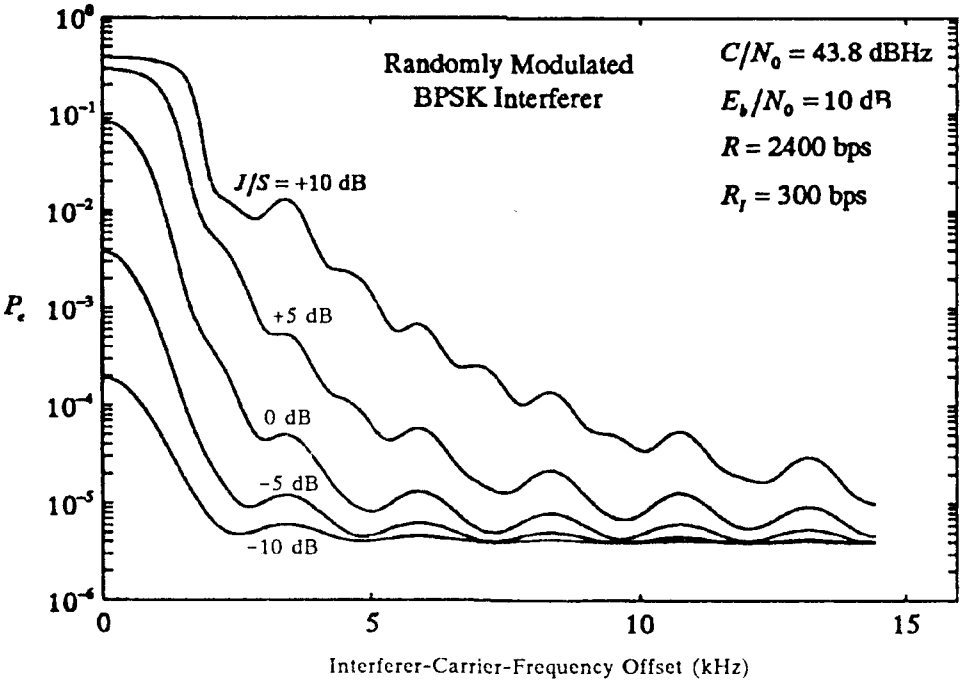

Figure 12. Probability of bit error vs. interferer-carrier-frequency offset, $R_I = R/2^3$.

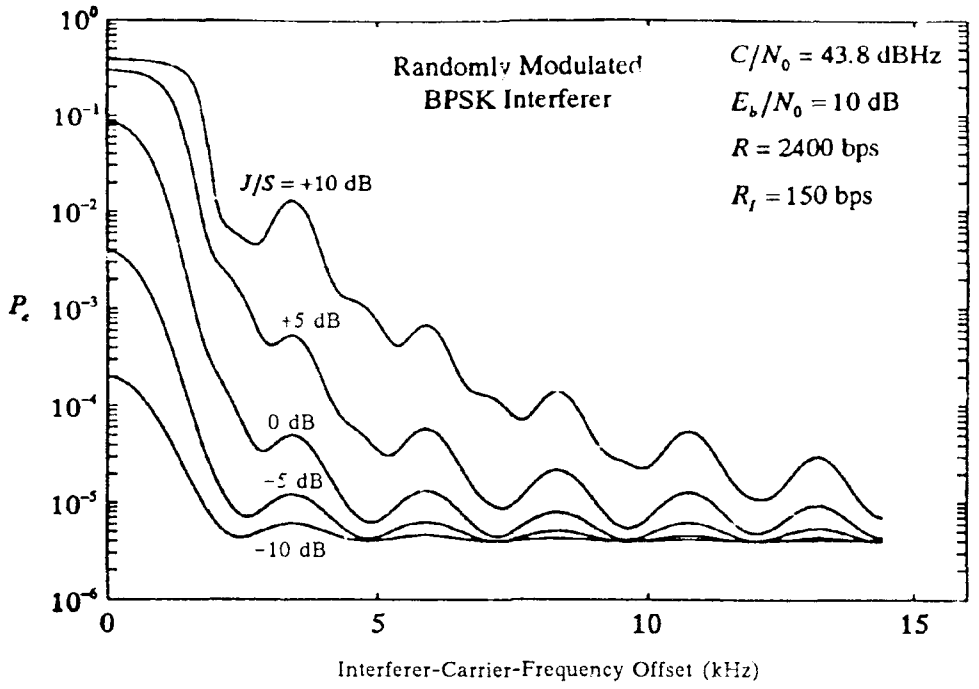

Figure 13. Probability of bit error vs. interferer-carrier-frequency offset, $R_I = R/2^4$.

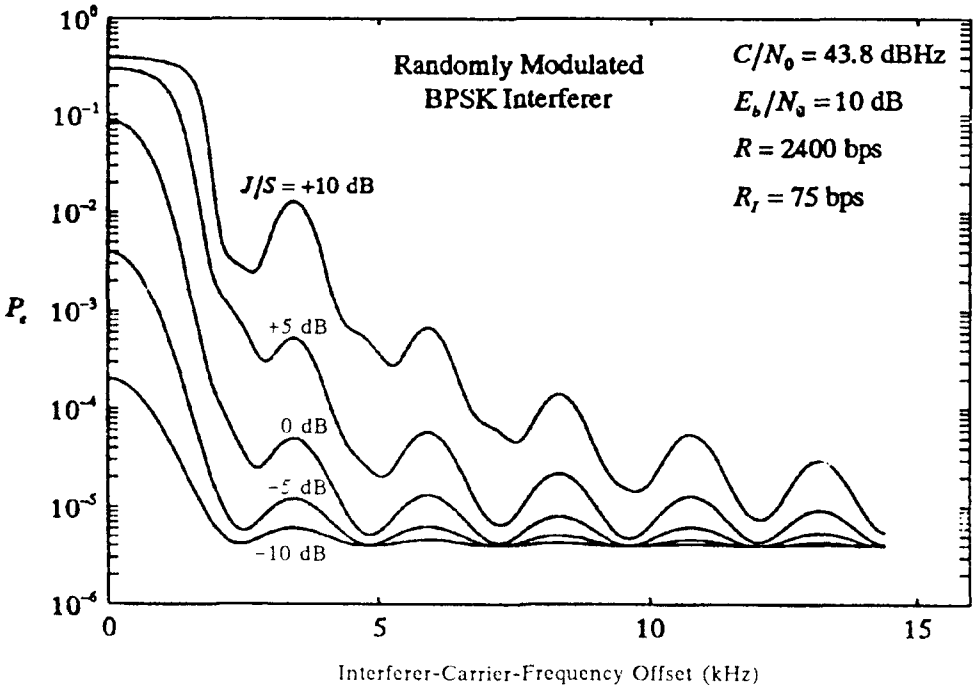

Figure 14. Probability of bit error vs. interferer-carrier-frequency offset, $R_I = R/2^5$.

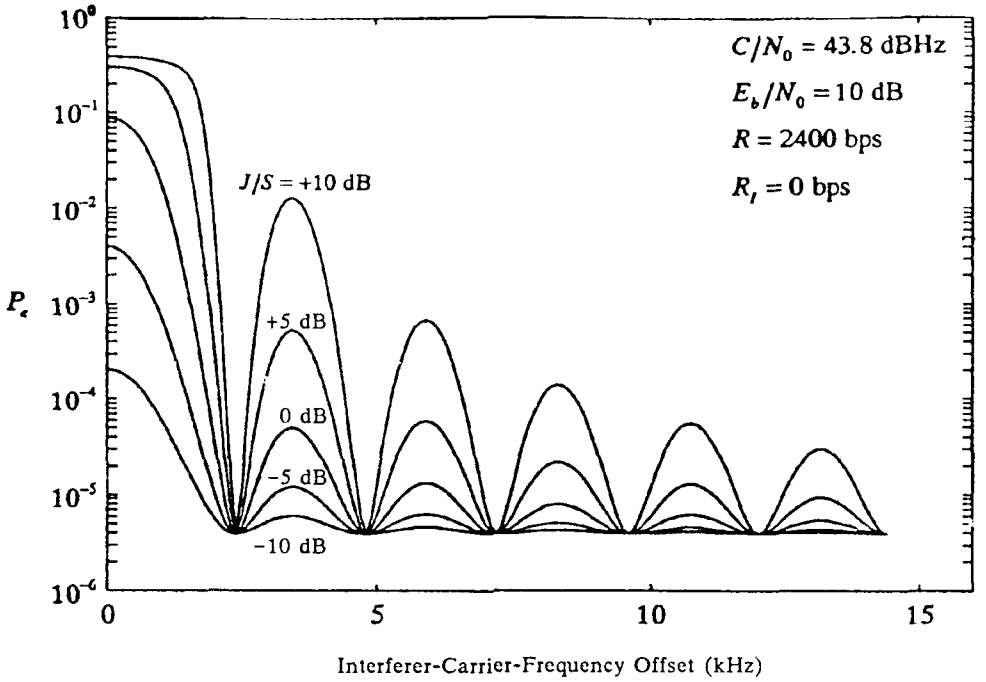

Figure 15. Probability of bit error vs. interferer-carrier-frequency offset, $R_I = 0$.

4.3 HIGHER DATA RATE BPSK INTERFERER

When $R_I > R$, there will be interfering signal bit transitions during all of the desired signal bit intervals [0, T]. This is shown at baseband in figure 16 for the case $R_I = 4R$ ($n = 2$ and $L = 3$ in eq. (17)) and $d_{-1} = d_1 = d_3 = -1, d_0 = d_2 = +1$. Let $I(T)$ denote the interferer component of $z(T)$, which is the second term in eq. (18). Then, carrying out the indicated integration,

$$
\begin{aligned}
I(T) \;=\; & A_I \frac{\cos\theta}{\delta}\{d_{-1}\sin\delta T + \sum_{k=0}^{L-1} d_k[\sin\delta(\tau + (k+1)T_I) - \sin\delta(\tau + kT_I)] \\
& + d_L(\sin\delta T - \sin\delta(\tau + LT_I))\} \\
& + A_I \frac{\sin\theta}{\delta}\{d_{-1}(\cos\delta\tau - 1) + \sum_{k=0}^{L-1} d_k[\cos\delta(\tau + (k+1)T_I) - \cos\delta(\tau + kT_I)] \\
& + d_L(\cos\delta T - \cos\delta(\tau + LT_I))\}
\end{aligned}
\tag{34}
$$

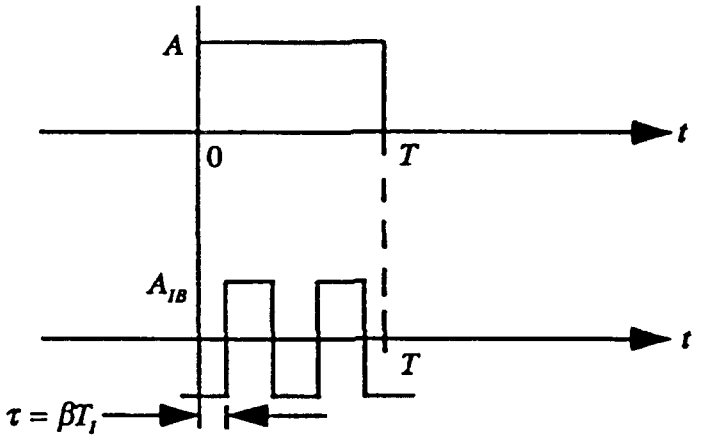

Figure 16. Desired (top) and interfering baseband signals in $[0, T]$, $R_I = 4R$, $d_{-1} = d_1 = d_3 = -1$, $d_0 = d_2 = +1$. $\tau = \beta T_I$, $0 \leq \beta < 1$.

Now, since $R_I = 2^n R$, for $\tau \neq 0$ there are $M = 2^{(2^n+1)} = 2^{(L+2)}$ possible interfering bit combinations. Values of M for $n = 1, 2, 3$, and 4 are listed in table 1.

Table 1. Number M of possible interfering bit combinations when $R_I = 2^n R$ and $\tau \neq 0$.

n	M
1	8
2	32
3	512
4	131,072

Let I_k denote the value of $I(T)$ evaluated using eq. (34) for the k^{th} (of M) combination of interfering bits. Then, if all interfering bit combinations are equally likely, the conditional probability of error, given the parameters of the interfering signal, is given by

$$P_e(A_I, \delta, \tau, \theta, n) = \frac{1}{M} \sum_{k=1}^{M} \Phi\left(\frac{-AT + I_k}{\sqrt{N_0 T}}\right). \tag{35}$$

As in eq. (29), the dependence on both θ and τ can be averaged out as follows

$$P_e(A_I, \delta, n) = \frac{1}{2\pi} \frac{1}{T_I} \int_0^{2\pi} d\theta \int_0^{T_I} d\tau \, P_e(A_I, \delta, \tau, \theta, n) \tag{36}$$

where θ and τ have been assumed to be mutually independent and uniformly distributed on $[0, 2\pi]$ and $[0, T_I]$ respectively.

4.3.1 Interferer-Carrier Frequency the Same as the Desired Signal-Carrier Frequency

Taking the limit of eq. (34) as the carrier-frequency offset δ goes to zero yields

$$\begin{aligned} \lim_{\delta \to 0} I(T) &= A_I \cos\theta \left\{ (d_{-1} - d_L)\tau + T_I \sum_{k=0}^{L} d_k \right\} \\ &= A_I T_I \cos\theta \left\{ (d_{-1} - d_L)\beta + \sum_{k=0}^{L} d_k \right\} \end{aligned} \tag{37}$$

using $T = 2^n T_I$, $L = 2^n - 1$, and $\tau = \beta T_I$ $(0 \le \beta < 1)$ for $R_I > R$. Substituting eq. (37) into eq. (18) yields the conditional expected value of the test statistic for the case of identical desired signal and interferer-carrier frequencies

$$E[z(T)|A_I, \beta, \theta, n] = \pm AT + A_I T_I \cos\theta \left\{ (d_{-1} - d_L)\beta + \sum_{k=0}^{L} d_k \right\}. \tag{38}$$

Figure 17 contains plots of the probability of bit error versus interferer-to-signal ratio, J/S, defined in eq. (33), calculated with eq. (36) using eq. (38), for BPSK interferer bit rates of $2R$ and $4R$ respectively, where R = 2400 bps. The integrations indicated in eq. (36) were performed numerically at each value of J/S. For the purpose of comparison, the CW interferer result plotted in figure 5 is also included in figure 17. With reference to table 1, exact evaluations of eq. (36) for $n \ge 3$ will not be presented here. The trend of decreasing P_e for increasing data rate BPSK interferers shown in figure 17 would continue as R_I is further increased. This is because the percentage of the possible interfering bit combinations that are most likely to cause an error decreases as R_I increases. Also, the results plotted were calculated under the assumption that all possible interfering bit combinations are equally likely. This assumption becomes less appropriate as the interfering-data rate increases. A string of consecutive identical interfering bits has the greatest impact on the probability of bit error in the BPSK system of interest. In many practical BPSK systems, the probability of an occurrence of N consecutive identical bits decreases as N increases due to the actions of data randomizers that attempt to keep such occurrences to a minimum in the transmitted signal (Ivanek, 1989, p. 216). Therefore, the BPSK interferer plots in figure 17 may be considered to be upper bounds (worst case) on the P_e performance of practical BPSK systems in the presence of BPSK interference.

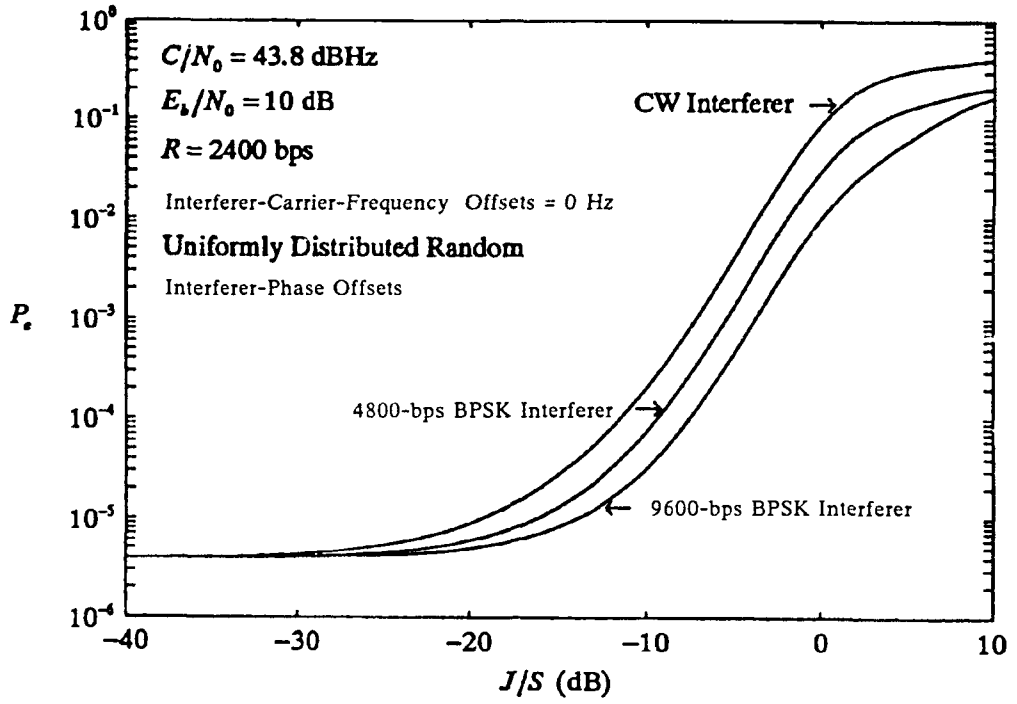

Figure 17. Probability of bit error vs. interferer-to-signal carrier power ratio, CW, 4800-bps and 9600-bps BPSK interferers.

4.3.2 Interferer-Carrier Frequency Different from the Desired Signal-Carrier Frequency

Figures 18 and 19 contain plots of eq. (36) evaluated for interferer-data rates of 4800 and 9600 bps respectively, when the interferer-carrier-frequency offset $\delta \neq 0$. Each figure contains a plot of eq. (36) for each of five values of J/S: +10, +5, 0, −5, and −10 dB. The integrations indicated in eq. (36) were performed numerically at each value of δ. As in figure 17, these curves were calculated under the assumption that all combinations of interfering bits are equally likely. Therefore, they can be considered to represent worst case performance. As expected, the higher data rate interferer will cause significant degradation in the P_e performance of the system of interest at higher values of δ due to the larger width of the main lobe of its spectrum.

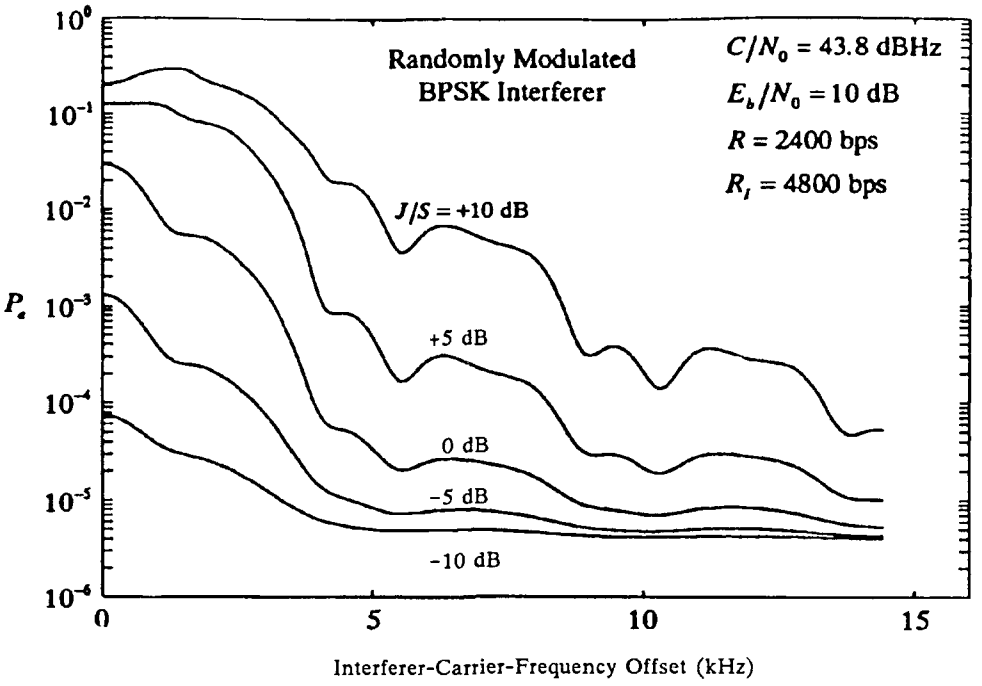

Figure 18. Probability of bit error vs. interferer-carrier-frequency offset, $R_I = 2R$.

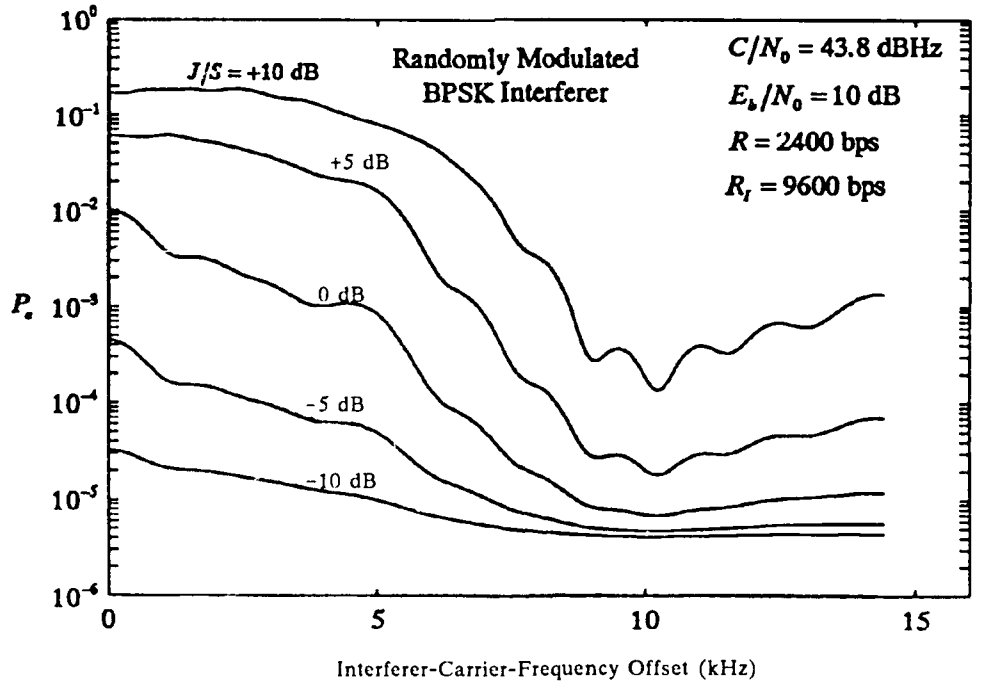

Figure 19. Probability of bit error vs. interferer-carrier-frequency offset, $R_I = 4R$.

5.0 EXTENSION TO DIFFERENTIALLY ENCODED BPSK

In this section, the results of the previous sections are extended to differentially encoded, coherently detected BPSK signals. Coherent detection of differentially encoded BPSK signals is used in the Navy UHF FLTSATCOM system (Naval Ocean Systems Center, 1991). An interesting interference-related consequence of the use of differential encoding occurs when the AN/WSC-3 UHF transceiver's transmitter is keyed with the input data line held at a constant logical "1" level.

In the previous sections it was assumed that a noise-free phase reference was available for coherent detection of the received BPSK signal. In the absence of interference, this results in a probability of bit error (or symbol error in a binary system) P_e given by

$$P_e = \Phi\left(-\sqrt{\frac{2E_b}{N_0}}\right) \tag{39}$$

as derived in section 2. In practice, a somewhat noisy phase reference is derived from the received signal by means of a carrier-tracking loop (Lindsey & Simon, 1973; Sklar, 1988, chapter 8; Viterbi, 1966; Zeimer & Peterson 1985). If the noise bandwidth of the tracking loop is on the order of 1 to 10 percent of the symbol bandwidth (considered to be a "narrowband" loop), then eq. (39) gives a very accurate indication of the "raw" symbol error probability of the system. Nonetheless, the possibility of phase ambiguity exists. That is, which phase corresponds to a logical "0" and which to a logical "1"? This ambiguity is often resolved in practical systems by the use of differential encoding.

5.1 DIFFERENTIALLY ENCODED BPSK

The term differential encoding implies that the presence of a logical "1" or "0" is manifested in the transmitted signal by a symbol's similarity to, or difference from, the preceding symbol. An example of differential encoding is presented in figure 20. In this example, the presence of a logical "1" is represented by a change in the transmitted phase. A logical "0" is represented by no change in the transmitted phase. In coherent detection of differentially encoded BPSK, the phase reference is derived from the received signal in the same manner as that employed for coherent BPSK described above. Thus, the "raw" symbol error probability of the scheme is given by eq. (39). A bit will be incorrectly detected if a correct symbol is followed by an incorrect symbol detection, or vice versa. Let $P_{e,d}$ denote the probability of bit error for coherent detection of differentially encoded BPSK. Then, with P_e given by eq. (39), we have

$$P_{e,d} = (1-P_e)P_e + P_e(1-P_e) = 2P_e(1-P_e) = 2P_e - 2P_e^2 \approx 2P_e. \tag{40}$$

A:		1	0	1	0	0	0	1	0	0	1	1	1	0	1	1	0	0
B:	0	π	π	0	0	0	0	π	π	π	0	π	0	0	π	0	0	0
C:	0	π	π	0	π	0	0	π	π	0	π	π	0	0	0	0	0	0
D:		1	0	1	1	1	0	1	0	1	1	0	1	0	0	0	0	0

A: Information Sequence
B: Transmitted Carrier Phase (initial phase arbitrary, 0 was selected)
C: Detected Carrier Phase (with 4 symbol errors)
D: Detected Information Sequence (with 6 bit errors resulting from errors in line "C")

Figure 20. An example of differentially encoded BPSK.

Thus, in coherent detection of differentially encoded BPSK, the bit-error rate is roughly twice the raw symbol-error rate of the system. Therefore, the results of the previous sections apply to the probability of bit error using coherent detection of differentially encoded BPSK within a factor of 2 as indicated in eq. (40). The bit-error rate performance of coherent detection of differentially encoded BPSK is compared to the performance of ideal coherent BPSK in figure 21. For typical error rates, the difference is less than 1 dB.

5.2 SQUARE-WAVE-MODULATED BPSK INTERFERER

The AN/WSC-3 UHF transceiver is widely deployed on ships and in shore stations of the Navy UHF FLTSATCOM system (Naval Ocean Systems Center, 1991). Differential encoding (decoding) is employed in the transmitter (receiver) section of the AN/WSC-3. Because of the use of differential encoding, if the transmitter is keyed when the input data line is in a static c dition, it will, depending on the level of the input data line, transmit either CW carrier w h no phase modulation, or alternating 0, 180-degree square-wave-phase modulation, at the selected bit rate. If an AN/WSC-3 is inadvertently left in this condition, it is effectively transmitting either a CW or square-wave-modulated BPSK interferer on the network at the selected carrier frequency. The effects of CW interferers were addressed in section 3 and the effects of randomly modulated BPSK interferers were presented in section 4. In this section, the effects of square-wave-modulated BPSK interferers on a desired 2400-bps BPSK signal are calculated.

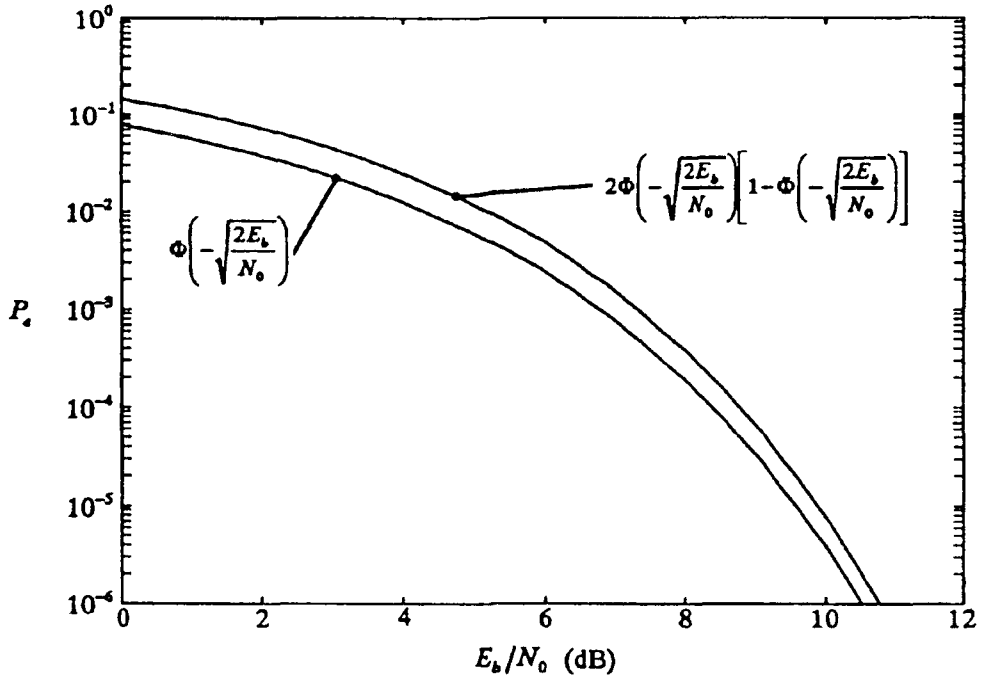

Figure 21. Probability of bit error for ideal coherent BPSK and coherent detection of differentially encoded BPSK vs. E_b/N_0.

In considering the effects of a square-wave-modulated BPSK signal interfering with a desired, randomly modulated BPSK signal, it is helpful to plot the frequency spectra of the two signals. If the data rate of the AN/WSC-3 that is the source of the interferer is selected to be $R_I = 1/T_I$, then the fundamental period of the interferer (at baseband) is $2T_I$. Since the square wave is periodic, it can be represented by a Fourier series and its spectrum consists of a set of lines. At baseband, the Fourier series $i(t)$ of the interferer is given by (Van Valkenburg, 1974, p. 458)

$$i(t) = \frac{4A_I}{\pi}\left[\cos(2\pi(R_I/2)t) - \frac{1}{3}\cos(2\pi(3R_I/2)t) + \frac{1}{5}\cos(2\pi(5R_I/2)t) - \frac{1}{7}\cos(2\pi(7R_I/2)t) + \cdots\right]. \tag{41}$$

At RF, the interferer spectrum consists of a symmetrical set of lines, centered at the carrier frequency, f_c, representing the positive and negative frequency components of the cosine terms in the Fourier series, eq. (41). This is illustrated in figure 22 for the case $R_I = R$ and identical interferer and desired signal-carrier frequencies ($\delta = 0$ in eq. (16)). The amplitude spectrum of the desired signal has been approximated by $|\text{sinc}((f - f_c/R)|$ where $\text{sinc}(f) = (\sin\pi f)/\pi f$.

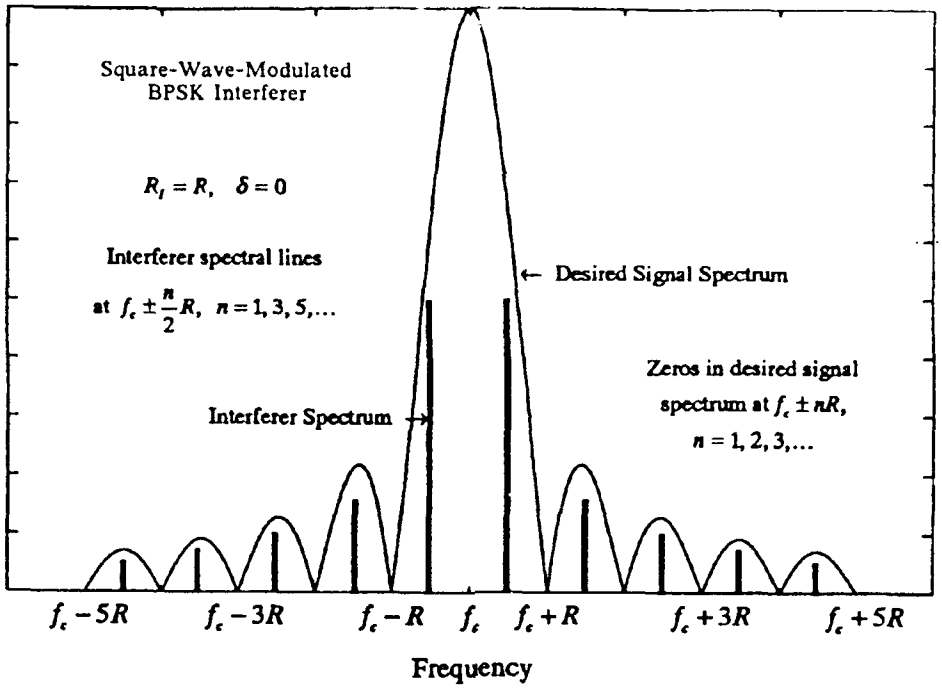

Figure 22. Interferer and desired signal amplitude spectra, $R_I = R, \delta = 0$.

5.2.1 Equal or Lower Data Rate Square-Wave-Modulated BPSK Interferer

When there is an interfering signal bit transition during the desired signal-bit interval (see figure 7), the conditional probability of bit error is given by a modified version of eq. (22). In the case of a square-wave-modulated BPSK interferer, there are only two possible outcomes vice the four outcomes for a randomly modulated BPSK interferer. These are (see figure 7) $\{d_{-1} = -1, d_0 = +1\}$ and $\{d_{-1} = +1, d_0 = -1\}$. Thus, when there is a bit transition of the square-wave-modulated interferer within [0, T], we have

$$P_e(A_I, \delta, \tau, \theta) = \frac{1}{2}\Phi\left(\frac{-AT - A_I K_1 + A_I K_2}{\sqrt{N_0 T}}\right) + \frac{1}{2}\Phi\left(\frac{-AT + A_I K_1 - A_I K_2}{\sqrt{N_0 T}}\right) \qquad (42)$$

where K_1 and K_2 are defined in eq. (21). The discussion in section 4.2 leading from eq. (26) to eq. (29) also applies here with $P_e(A_I, \delta, \tau, \theta)$ calculated according to eq. (42) vice eq. (22). When $\tau = 0$, eq. (42) reduces to the CW interferer result in eq. (11), again with α replaced by A_I. Thus, the effect of an equal or lower data rate square-wave-modulated BPSK interferer can be calculated using eqs. (29) and (42).

5.2.1.1 Interferer-Carrier Frequency the Same as the Desired Signal-Carrier Frequency. When $\delta = 0$, K_1 and K_2 are again given by eq. (30). Substituting eq. (30) into eq. (42) yields

$$P_e(A_I, \beta, \theta) = \frac{1}{2}\Phi\left(\frac{-T(A + A_I[2\beta - 1]\cos\theta)}{\sqrt{N_0 T}}\right) + \frac{1}{2}\Phi\left(\frac{-T(A - A_I[2\beta - 1]\cos\theta)}{\sqrt{N_0 T}}\right) \quad (43)$$

which corresponds to eq. (32) for the case of a randomly modulated BPSK interferer. Figure 23 shows eq. (43) plotted versus β for $\theta = 0$ for four values of J/S. Figure 23 should be compared to figure 8. When the interfering modulation consists of a square wave, it effectively cancels itself out when its bit transition occurs in the middle of the desired signal-bit interval. Figure 24 contains plots of eq. (29) evaluated for $\gamma = 1$ and $\gamma = 0$ using eq. (43). The integrations over τ and θ indicated in eq. (29) were performed numerically at each value of J/S. The two curves in figure 24 bound the effects of the interference caused to an $R = 2400$ bps desired BPSK signal by a square-wave-modulated BPSK interferer with interfering data rate R_I in the range $0 \leq R_I \leq 2400$ bps.

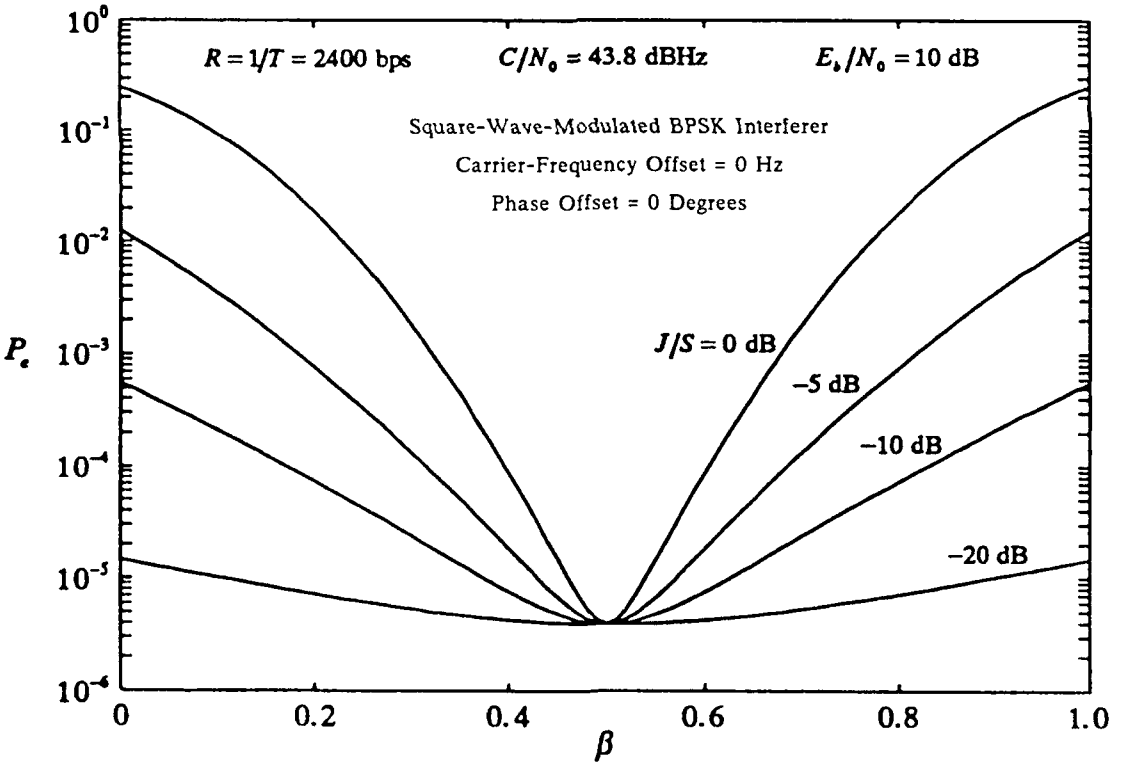

Figure 23. Probability of bit error as a function of the position of a single interfering signal-bit transition in $[0, T]$ when the interferer consists of a square-wave-modulated BPSK signal. $\beta = \tau/T$ (see also figures 7 and 8). $J/S = 0$, −5, −10, −20 dB.

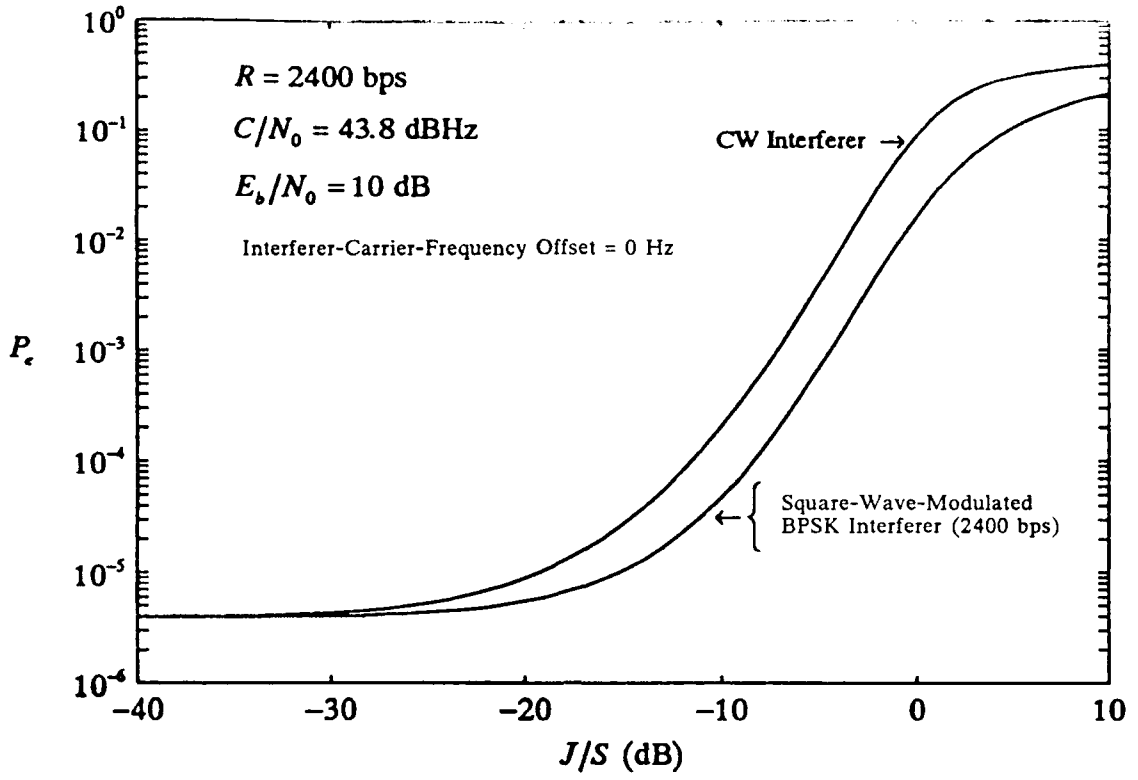

Figure 24. Probability of bit error vs. interferer-to-signal carrier power ratio, CW interferer and 2400-bps square-wave-modulated BPSK interferer.

5.2.1.2 Interferer-Carrier Frequency Different from the Desired Signal-Carrier Frequency. Figures 25 through 30 contain plots of eq. (29) using eq. (42) evaluated for square-wave-modulated BPSK interferer-data rates of 2400, 1200, 600, 300, 150, and 75 bps respectively, when the interferer-carrier-frequency offset $\delta \neq 0$. In all cases, the desired signal-data rate is 2400 bps. Each figure contains a plot of eq. (29) using eq. (42) for each of five values of J/S: +10, +5, 0, −5, and −10 dB. The integrations indicated in eq. (29) were performed numerically for each value of δ. Again, as indicated by eq. (40), the bit-error rate performance shown in figures 25 to 30 applies to coherent detection of differentially encoded BPSK within a factor of 2.

5.2.2 Higher Data Rate Square-Wave-Modulated BPSK Interferer

When the data rate of the square-wave-modulated BPSK interferer is greater than that of the desired, randomly modulated BPSK signal ($R_I = 2^n R, n \geq 1$), there will always be bit transitions of the interfering signal within the desired signal-bit time [0, T]. However, whether or not there will be any interference with the desired signal is completely determined by the offset δ of the interferer-carrier frequency from the carrier frequency, f_c, of the desired signal. In figures 31 and 32, the spectra of the desired signal and that of

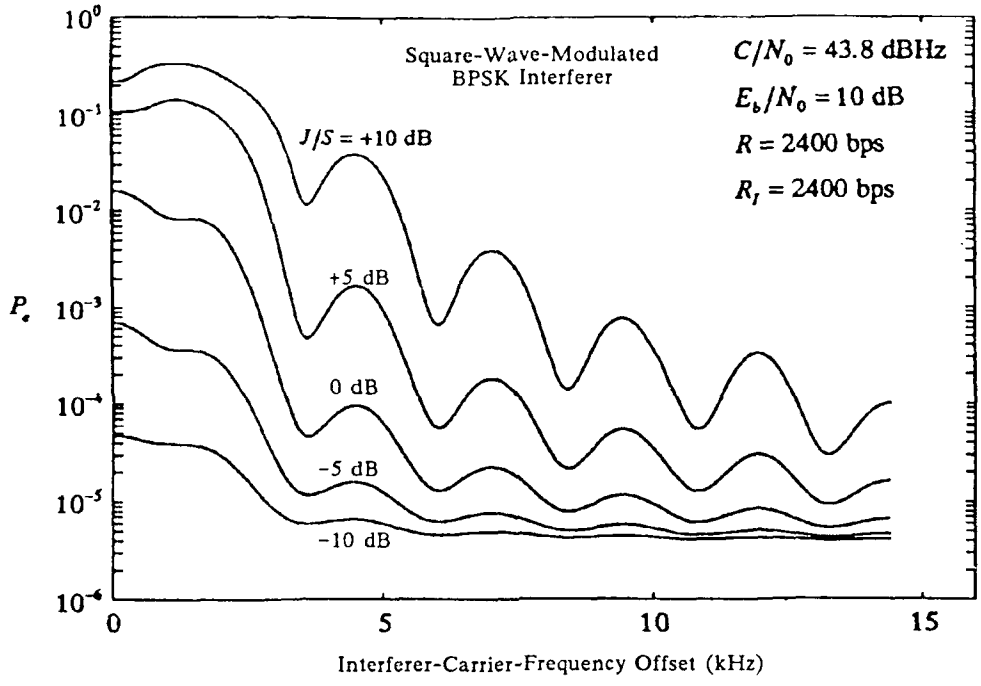

Figure 25. Probability of bit error vs. interferer-carrier-frequency offset, $R_I = R$.

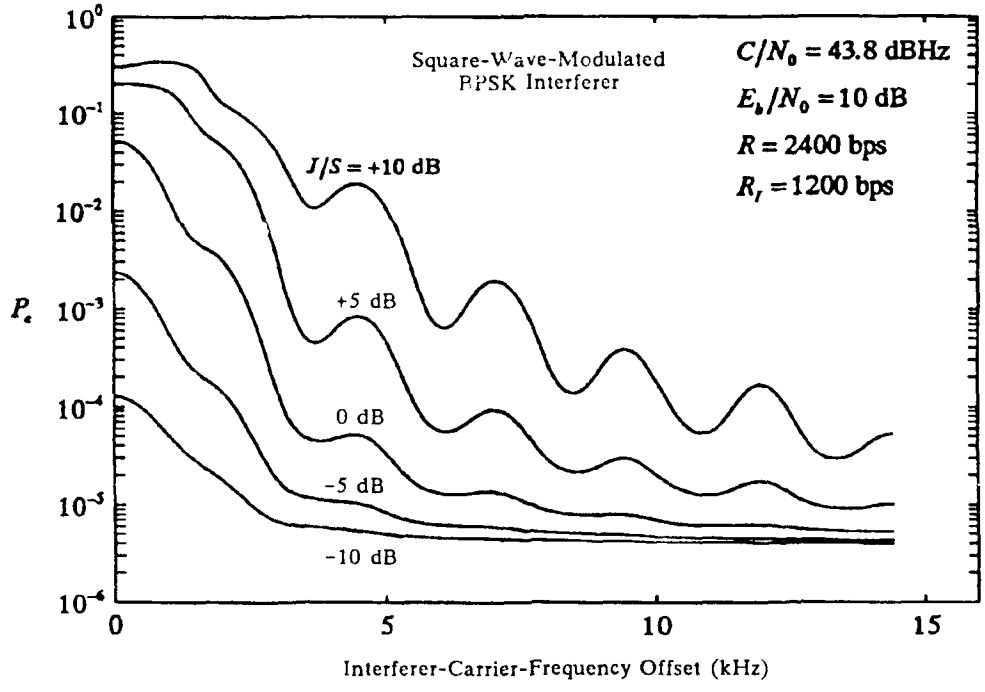

Figure 26. Probability of bit error vs. interferer-carrier-frequency offset, $R_I = R/2$.

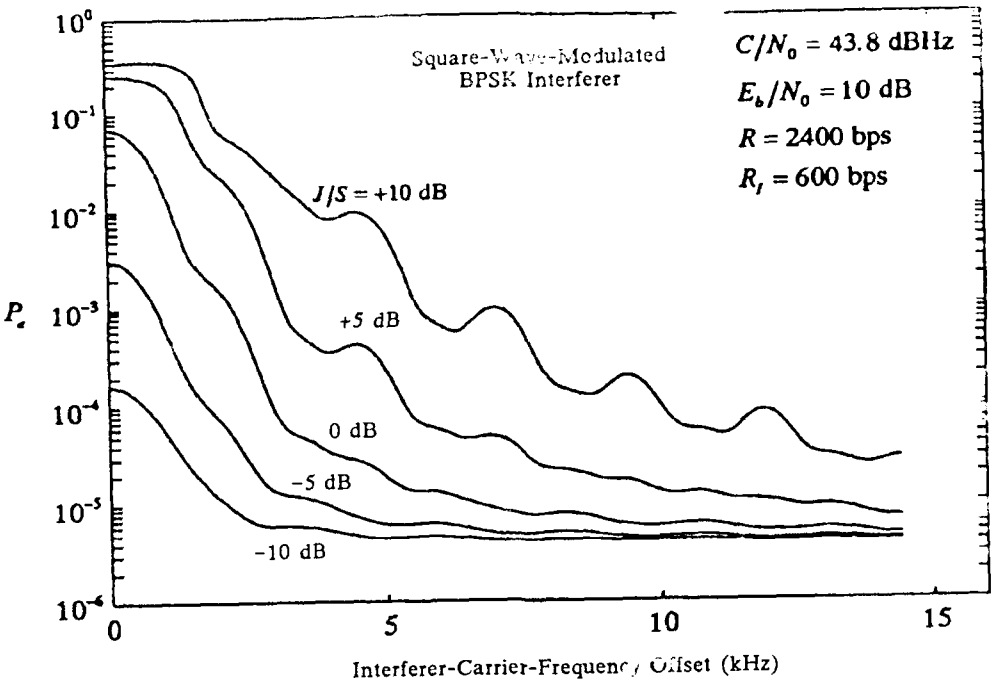

Figure 27. Probability of bit error vs. interferer-carrier-frequency offset, $R_I = R/2^2$.

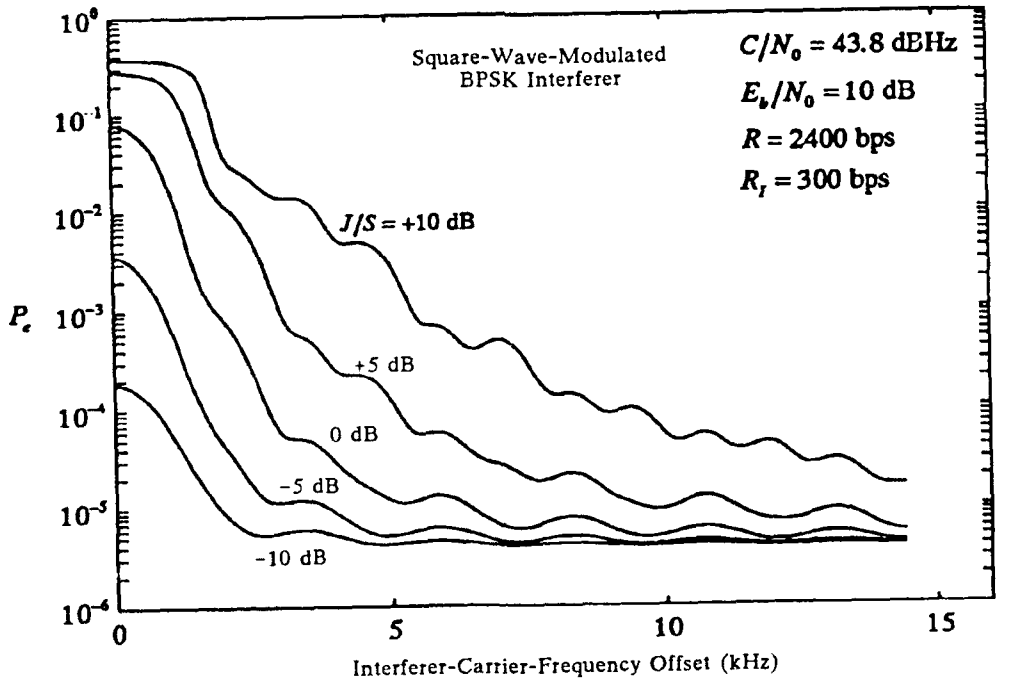

Figure 28. Probability of bit error vs. interferer-carrier-frequency offset, $R_I = R/2^3$.

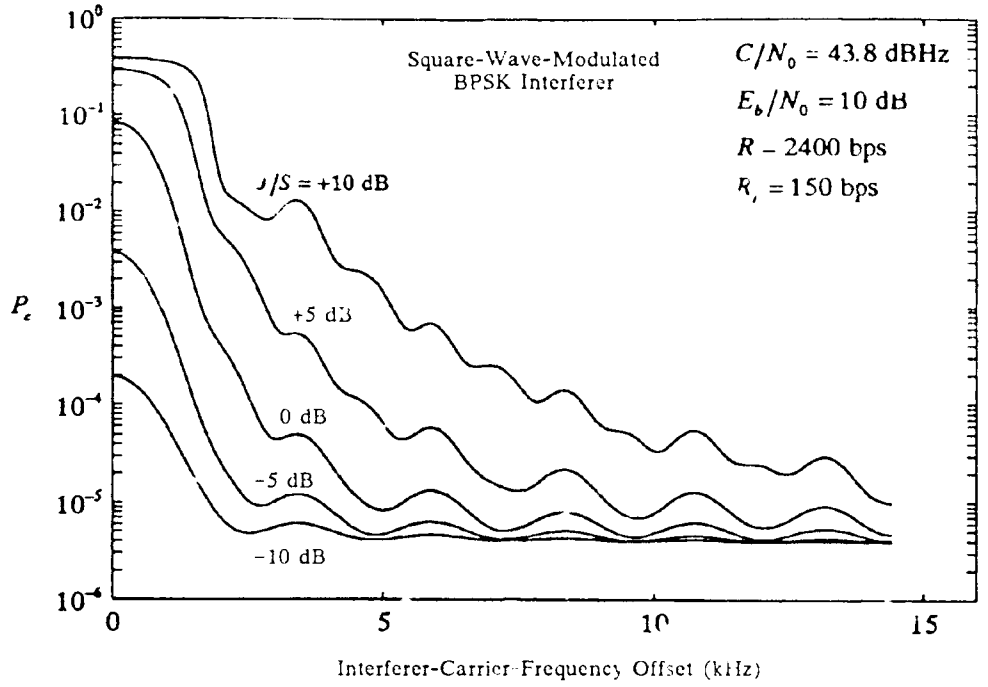

Figure 29. Probability of bit error vs. interferer-carrier-frequency offset, $R_I = R/2^7$.

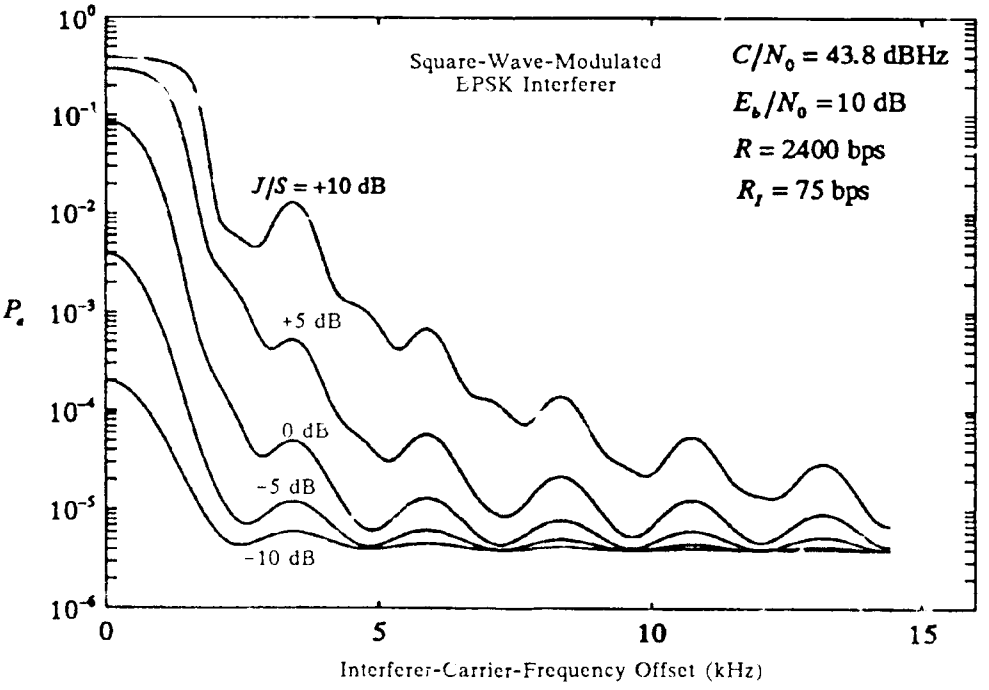

Figure 30. Probability of bit error vs. interferer-carrier-frequency offset, $R_I = R/2^5$.

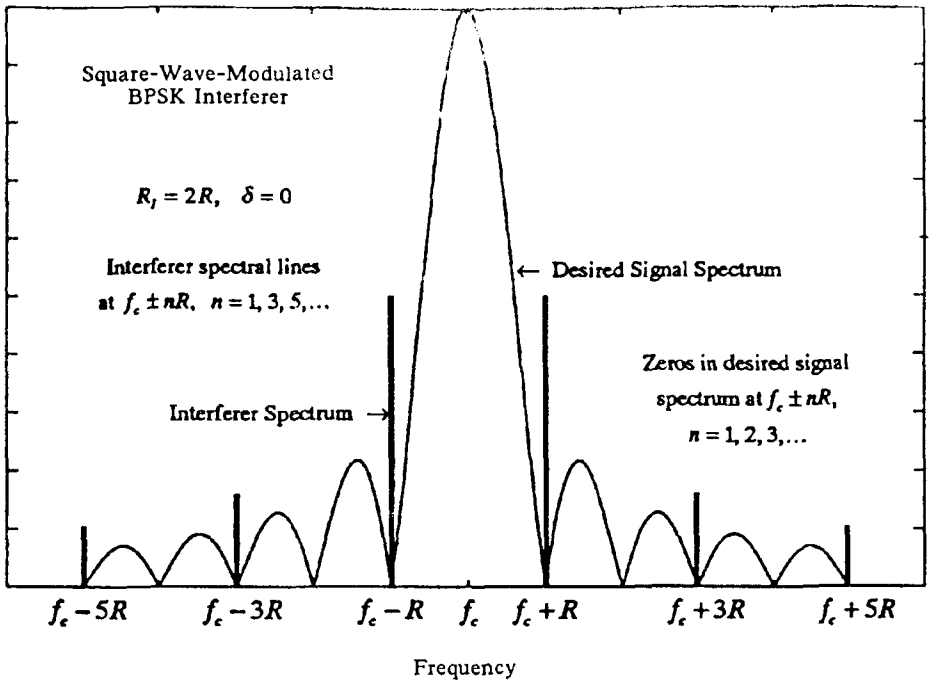

Figure 31. Interferer and desired signal-amplitude spectra, $R_I = 2R, \delta = 0$.

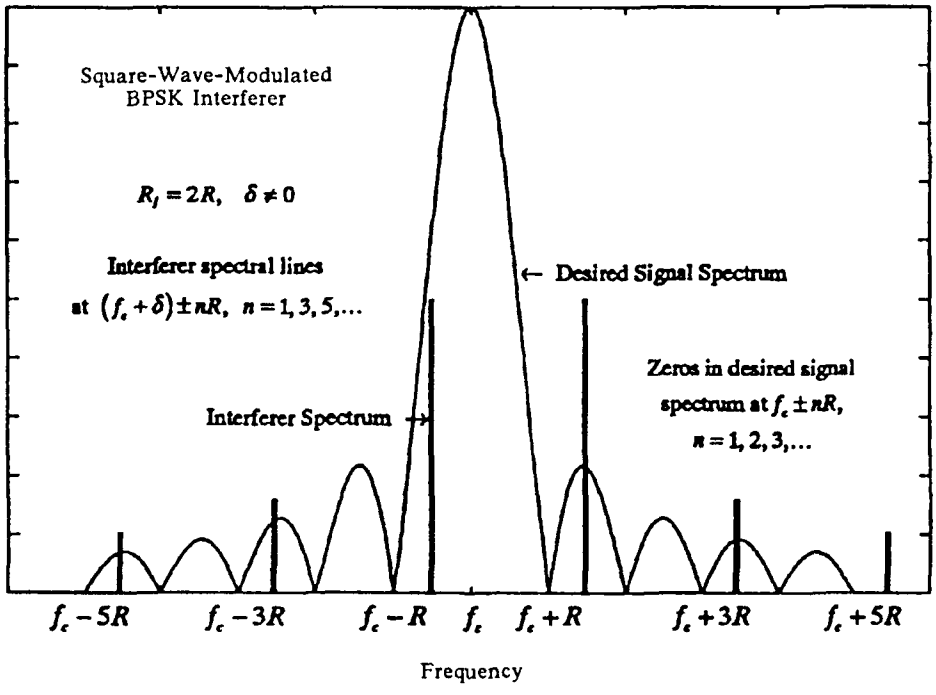

Figure 32. Interferer and desired signal-amplitude spectra, $R_I = 2R, \delta \neq 0$.

a square-wave-modulated BPSK interferer, $R_I = 2R$, are illustrated for cases in which $\delta = 0$ and $\delta \neq 0$ respectively. From figure 31, it is apparent there will be no interference when $\delta = 0 \pm 2mR, m = 0, 1, 2, \ldots$, in an ideal system. From figure 32, it is apparent that when $\delta \neq 0 \pm 2mR$, there will be interference with the desired signal.

As in section 4.3, the interferer component of the test statistic $z(T)$ is given by eq. (34). Here, however, since the interferer modulation is a square wave and not random, there are only two possible combinations of interfering bits for all values of $n \geq 1$ in $R_I = 2^n R$. (See table 1 for a randomly modulated BPSK interferer.) For $n = 1$ these are

$$\{d_{-1} = -1, d_0 = +1, d_1 = -1\} \text{ and } \{d_{-1} = +1, d_0 = -1, d_1 = +1\} \tag{44}$$

For $n = 2$ they are

$$\begin{aligned} &\{d_{-1} = -1, d_0 = +1, d_1 = -1, d_2 = +1, d_3 = -1\} \text{ and} \\ &\{d_{-1} = +1, d_0 = -1, d_1 = +1, d_2 = -1, d_3 = +1\}. \end{aligned} \tag{45}$$

Figure 33 contains a plot of eq. (36) evaluated as a function of interferer-carrier-frequency offset δ at the five indicated values of J/S for the case $R_I = 2R$. Here eq. (35) was used in eq. (36) with $M = 2$, and the two values of I_k were determined by using eq. (44) in eq. (34). The assertion made above regarding the values of δ for which there will be no interference is confirmed in figure 33.

Figure 34 contains plots of the desired signal and interfering signal spectra for the case $R_I = 4R$ and $\delta = 0$. From figure 34, it can be seen that there will be no interference when $\delta = 0 \pm jR$ for integer j, except when $j = 2, 6, 10, \ldots = n + \ell 2^n, \ell = 0, 1, 2, \ldots$. (Here $n = 2$. The formula also applies in general, including above for $n = 1$.) Figure 35 contains a plot of eq. (36) evaluated as a function of interferer-carrier-frequency offset δ at the five indicated values of J/S for the case $R_I = 4R$. Here eq. (35) was used in eq. (36) with $M = 2$, but with the two values of I_k determined by using eq. (45) in eq. (34). Again, the values of δ for which there will be no interference are accurately predicted from the spectral plots. And, as indicated by eq. (40), the bit-error-rate performance shown in figures 33 and 35 applies to coherent detection of differentially encoded BPSK within a factor of 2.

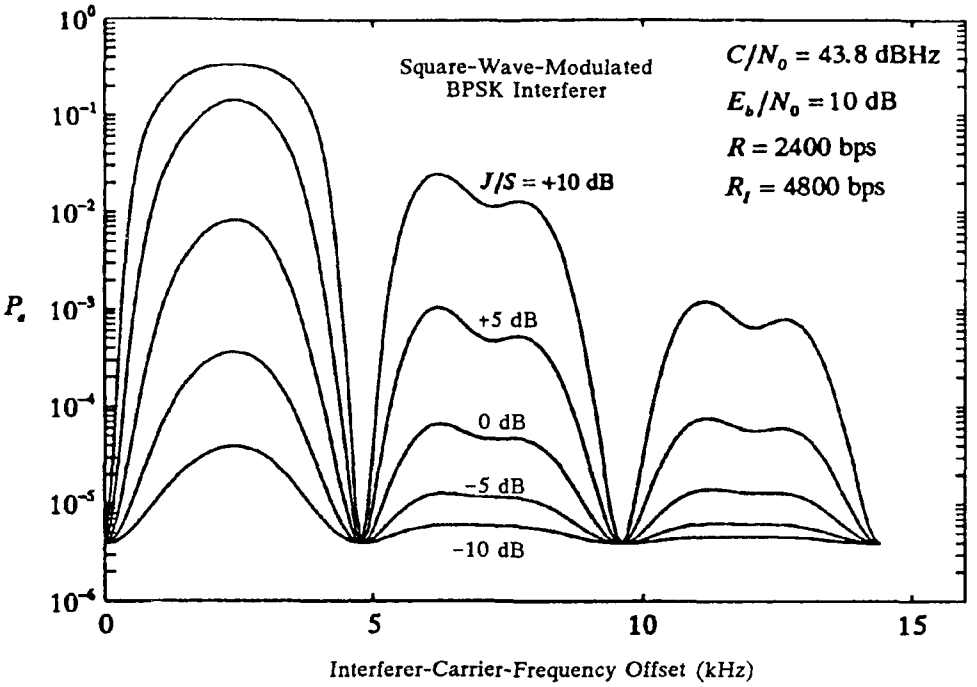

Figure 33. Probability of bit error vs. interferer-carrier-frequency offset, $R_I = 2R$.

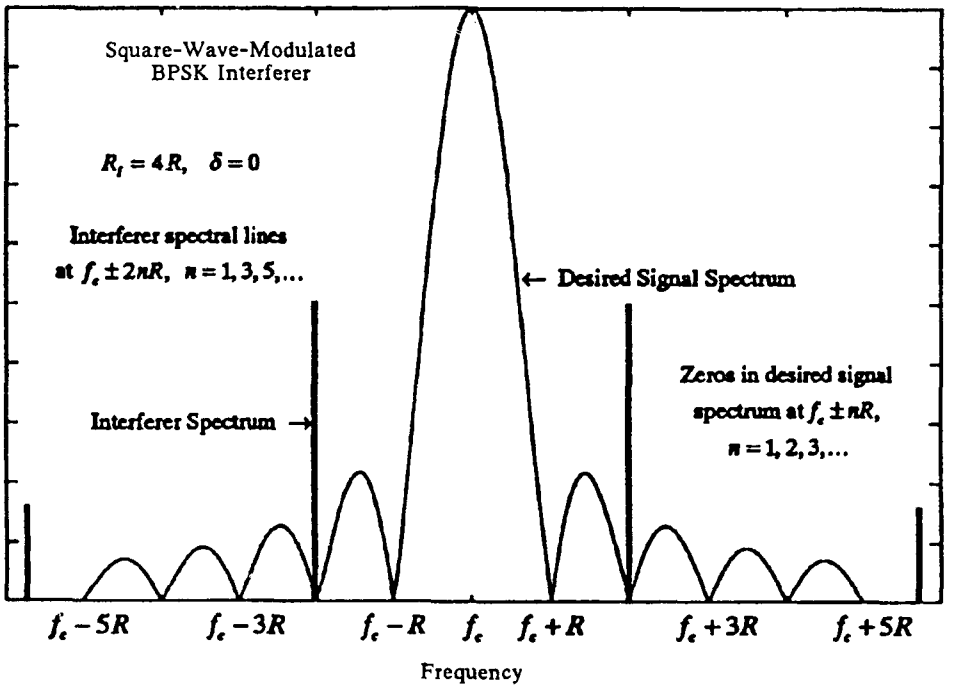

Figure 34. Interferer and desired signal-amplitude spectra, $R_I = 4R, \delta = 0$.

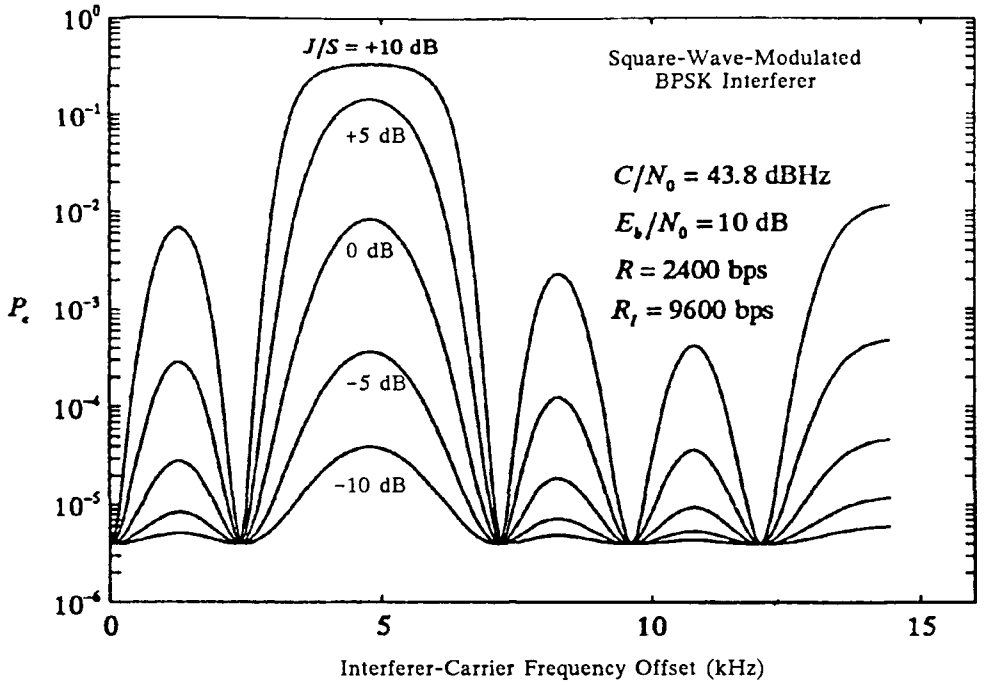

Figure 35. Probability of bit error vs. interferer-carrier-frequency offset, $R_I = 4R$.

6.0 CONCLUSION

To measure the success of any scheme to reduce the effects of interference, it is important to know what the effects of the interference would be if mitigating techniques were not used. The calculations made in this report are those of CW- and BPSK-signal interferers on a standard BPSK communications system. These are the same types of interferers found in many BPSK communications systems.

7.0 GLOSSARY

CW	continuous wave
BPSK	binary phase shift keyed
FEC	forward error correction
AWGN	additive white Gaussian noise
UHF	ultrahigh frequency
FLTSATCOM	Fleet satellite communications
J/S	interferer-to-signal carrier power ratio
P_e	Probability of bit error
dB	decibels
Hz	hertz
bps	bits per second
kHz	kilohertz
SNR	signal-to-noise ratio
dBHz	decibels-hertz
RF	radio frequency
C/N_0	carrier-to-noise density ratio
E_b/N_0	energy per bit-to-noise density ratio (SNR)
R	information rate
T	bit time
θ	interfering signal phase
δ	interfering signal-carrier-frequency offset
τ	bit transition time offset

8.0 REFERENCES

Helstrom, C. W. 1984. *Probability and Stochastic Processes for Engineers*, MacMillan Publishing Company, New York.

Ivanek, F. 1989. *Terrestrial Digital Microwave Communications*, Artech House, Norwood, MA.

Lindsey, W. C., and M. K. Simon, 1973. *Telecommunication Systems Engineering*, Prentice-Hall, Englewood Cliffs, New Jersey.

Milstein, L. B. 1991. Lecture notes for ECE 258A: Digital Communications, Department of Electrical and Computer Engineering, University of California at San Diego.

Naval Ocean Systems Center. 1991. *Navy UHF Satellite Communication System Description*, FSCS-200-83-1, 31 December.

Proakis, J. 1989. *Digital Communications-Second Edition*, McGraw-Hill, New York.

Schwartz, M. 1980. *Information Transmission, Modulation, and Noise-Third Edition*, McGraw-Hill, New York.

Sklar, B. 1988. *Digital Communications: Fundamentals and Applications*, Prentice-Hall, Englewood Cliffs, New Jersey.

Van Valkenburg, M. E. 1974. *Network Analysis-Third Edition*, Prentice-Hall, Englewood Cliffs, New Jersey.

Viterbi, A. J. 1966. *Principles of Coherent Communications*, McGraw-Hill, New York.

Viterbi, A. J. 1991. "Wireless Digital Communication: A View Based on Three Lessons Learned," *IEEE Communications Magazine*, pp. 33-36, September.

Ziemer, R. E., and R. L. Peterson. 1985. *Digital Communications and Spread Spectrum Systems*, MacMillan Publishing Company, New York.

Ziemer, R. E., and R. L. Peterson. 1992. *Introduction to Digital Communication*, MacMillan Publishing Company, New York.

REPORT DOCUMENTATION PAGE

Form Approved
OMB No. 0704-0188

iENCY USE ONLY *(Leave blank)*	2. REPORT DATE	3. REPORT TYPE AND DATES COVERED
	August 1992	Final: Oct 91 – Apr 92

LE AND SUBTITLE

'FECTS OF CW- AND BPSK-SIGNAL INTERFERENCE ON A STANDARD 'SK DIGITAL COMMUNICATIONS SYSTEM

5. FUNDING NUMBERS

PE: OMN
PROJ: CG48

ITHOR(S)

A. Axford

RFORMING ORGANIZATION NAME(S) AND ADDRESS(ES)

ıval Command, Control and Ocean Surveillance Center (NCCOSC)
)T&E Division (NRaD)
n Diego, CA 92152–5000

8. PERFORMING ORGANIZATION REPORT NUMBER

NRaD TR 1510

ONSORING/MONITORING AGENCY NAME(S) AND ADDRESS(ES)

ıace and Naval Warfare Systems Command
ıde 504P3
ashington, DC 20363–5100

10. SPONSORING/MONITORING AGENCY REPORT NUMBER

UPPLEMENTARY NOTES

DISTRIBUTION/AVAILABILITY STATEMENT

ıproved for public release; distribution is unlimited.

12b. DISTRIBUTION CODE

BSTRACT *(Maximum 200 words)*

This report contains calculations of the effects of CW- and BPSK-signal interferers on a standard BPSK mmunications system. These types of interferers are typical of those encountered in many BPSK communications systems.

IBJECT TERMS

tinuous wave (CW)
ary phase shift keyed (BPSK)
itive white Gaussian noise (AWGN)
forward error correction (FEC)
interferers

15. NUMBER OF PAGES
50

16. PRICE CODE

CURITY CLASSIFICATION REPORT	18. SECURITY CLASSIFICATION OF THIS PAGE	19. SECURITY CLASSIFICATION OF ABSTRACT	20. LIMITATION OF ABSTRACT
CLASSIFIED	UNCLASSIFIED	UNCLASSIFIED	SAME AS REPORT

INITIAL DISTRIBUTION

Code 0012	Patent Counsel	(1)
Code 0144	R. November	(1)
Code 144	V. Ware	(1)
Code 572	T. R. Albert	(1)
Code 751	R. Slack	(1)
Code 804	G. W. Parker	(5)
Code 804	J. R. Zeidler	(1)
Code 824	R. C. North	(1)
Code 824	J. Rockway	(1)
Code 824	C. Fuzak	(1)
Code 84	C. E. Gibbens	(1)
Code 842	J. Meenan	(1)
Code 843	D. Gookin	(1)
Code 844	R. A. Axford	(20)
Code 844	R. R. James	(1)
Code 844	J. Parsons	(1)
Code 844	R. Nies	(1)
Code 952B	J. Puleo	(1)
Code 961	Archive/Stock	(6)
Code 964B	Library	(2)

Defense Technical Information Center
Alexandria, VA 22304-6145 (4)

NCCOSC Washington Liaison Office
Washington, DC 20363-5100

Center for Naval Analyses
Alexandria, VA 22302-0268

Navy Acquisition, Research & Development
Information Center (NARDIC)
Washington, DC 20360-5000

Space & Naval Warfare Systems Command
Washington, DC 20363-5100 (3)